

Landscape of standing variation for tandem duplications in *Drosophila yakuba* and *Drosophila simulans*

Rebekah L. Rogers¹, Julie M. Cridland^{1,2}, Ling Shao¹, Tina T. Hu³,
Peter Andolfatto³, and Kevin R. Thornton¹

Research Article

- 1) Ecology and Evolutionary Biology, University of California, Irvine
- 2) Ecology and Evolutionary Biology, University of California, Davis
- 3) Ecology and Evolutionary Biology and the Lewis Stigler Institute for Integrative Genomics, Princeton University

Running head: Tandem duplications in non-model *Drosophila*

Key words: Tandem duplications, Deletions, *Drosophila yakuba*, *Drosophila simulans*, evolutionary novelty

Corresponding author: Rebekah L. Rogers, Dept. of Ecology and Evolutionary Biology, 5323 McGaugh Hall, University of California, Irvine, CA 92697

Phone: 949-824-0614

Fax: 949-824-2181

Email: rogersrl@uci.edu

Abstract

We have used whole genome paired-end Illumina sequence data to identify tandem duplications in 20 isofemale lines of *D. yakuba*, and 20 isofemale lines of *D. simulans* and performed genome wide validation with PacBio long molecule sequencing. We identify 1,415 tandem duplications that are segregating in *D. yakuba* as well as 975 duplications in *D. simulans*, indicating greater variation in *D. yakuba*. Additionally, we observe high rates of secondary deletions at duplicated sites, with 8% of duplicated sites in *D. simulans* and 17% of sites in *D. yakuba* modified with deletions. These secondary deletions are consistent with the action of the large loop mismatch repair system acting to remove polymorphic tandem duplication, resulting in rapid dynamics of gain and loss in duplicated alleles and a richer substrate of genetic novelty than has been previously reported. Most duplications are present in only single strains, suggesting deleterious impacts are common. *D. simulans* shows larger numbers of whole gene duplications in comparison to larger proportions of gene fragments in *D. yakuba*. *D. simulans* displays an excess of high frequency variants on the X chromosome, consistent with adaptive evolution through duplications on the *D. simulans* X or demographic forces driving duplicates to high frequency. We identify 78 chimeric genes in *D. yakuba* and 38 chimeric genes in *D. simulans*, as well as 143 cases of recruited non-coding sequence in *D. yakuba* and 96 in *D. simulans*, in agreement with rates of chimeric gene origination in *D. melanogaster*. Together, these results suggest that tandem duplications often result in complex variation beyond whole gene duplications that offers a rich substrate of standing variation that is likely to contribute both to detrimental phenotypes and disease, as well as to adaptive evolutionary change.

Introduction

Gene duplications are an essential source of genetic novelty that can be useful in adaptation and in the origins of developmental complexity across phyla (Conant and Wolfe 2008). Additionally, duplicate sequences are commonly found in mammalian stem cells (Liang et al. 2008), cancer cell lines (Inaki and Liu 2012), and are associated with autoimmune disease, HIV susceptibility, Crohn’s disease, asthma, allergies, and autism (Ionita-Laza et al. 2009). Distinguishing the propensity with which gene duplications serve as causative disease factors as opposed to a source of favorable variation depends heavily on accurate ascertainment of their occurrence and frequencies in the population.

In the *Drosophila* there is substantial variation in the number and types of duplicate genes that are present in the sequenced reference genomes (Hahn, Han and Han 2007), though the extent to which selection might drive rapid fixation of duplicate genes or whether mutation rates differ across species remains uncertain. Furthermore, these surveys of single strains from each species may not be representative of the variation present in populations and offer only limited opportunities to study their role in adaptation. The advent of Illumina sequencing has made population genomics of complex mutations in non-model *Drosophila* readily tractable. Paired-end Illumina sequencing offers the opportunity to survey copy number variation using definitive sequence-based comparisons that are free from complications related to sole use of coverage or hybridization intensities. Through the identification of paired-end reads that map in abnormal orientations, we can identify a high-confidence dataset describing tandem duplications in sample populations (Cridland and Thornton 2010, Korb et al. 2007, Tuzun et al. 2005).

D. yakuba and *D. simulans* offer the opportunity to compare the role of tandem duplications in species that have high levels of nucleotide diversity and large effective population sizes of $N_e \approx 10^6$ (Bachtrog et al. 2006, Sawyer and Hartl 1992, Eyre-Walker et al. 2002), allowing us to compare mutational and adaptive processes in independent systems where neutral forces of genetic drift should be minimal.

If different chromosomes produce tandem duplications at different rates, we may expect them to contribute differentially to adaptive changes. In *D. melanogaster*, the X chromosome contains greater repetitive content (Mackay et al. 2012), displays different gene density (Adams et al 2000), has potentially smaller population sizes (Wright 1931, Andolfatto 2001), lower levels of background selection (Charlesworth 2012), and an excess of genes involved in female-specific expression (Ranz et al. 2003) in comparison to the autosomes. Furthermore, the X chromosome is hemizygous in males, exposing recessive mutations to the full effects of selection more often than comparable loci on the autosomes (Charlesworth, Coyne and Barton 1987). Hence, the incidence of duplications on the X and the types of genes affected may differ from the autosomes, and thereby produce different impacts on phenotypic evolution.

Many copy number variants are thought to be non-neutral (Emerson et al. 2008, Cardoso-Moreira et al. 2011, Hu and Worton 1992), especially when they capture partial gene sequences or create chimeric gene structures (Rogers and Hartl 2012) or result in recruitment of non-coding sequences (Lee and Reinhardt 2012). Such modifications are

likely to change gene regulatory profiles (Rogers and Hartl 2012), increasing the likelihood of non-neutral phenotypes. Surveys in *D. melanogaster* have identified large numbers of such variants (Emerson et al. 2008, Cardoso-Moreira et al. 2011, Cardoso-Moreira, Arguello and Clark 2012, Lee and Reinhardt 2012, Rogers, Bedford and Hartl 2009). Establishing profiles of partial gene duplication, whole gene duplication, chimera formation, and recruitment of non-coding sequence are essential to a complete understanding of the roles tandem duplicates play in beneficial and detrimental phenotypic changes across species.

Here we describe the number, types, and genomic locations of tandem duplications segregating in 20 strains of *D. yakuba* and in 20 strains of *D. simulans* and discuss differences across species and across chromosomes, as well as their potential to create novel gene constructs.

Results

We have sequenced the complete genomes of 20 isofemale lines of *D. yakuba* and 20 isofemale lines *D. simulans* each inbred in the lab for 9-12 generations to produce effectively haploid samples, as well as the reference genome stocks of each species (as a control for genome quality and false positives) (Drosophila Twelve Genomes Consortium 2007, Hu et al. 2012). Genomes are sequenced to high coverage of 50-150X for a total of 42 complete genomes (Table S1-S5, see Methods). We have used mapping orientation of paired-end reads to identify recently-derived, segregating duplications in these samples less than 25 kb in length that are supported by 3 or more divergently-oriented read pairs (see Methods, Text S1, Table S6-S7). We limit analysis to regions of the genome which can be assayed with coverage depth of 3 or more reads across all strains, corresponding to the detection limit for tandem duplicates. We identify 1,415 segregating tandem duplications in *D. yakuba* and 975 segregating tandem duplications in *D. simulans* (Figure 1), including large numbers of gene duplications (Table 1) with a low false positive rate (Table S8). We assess the numbers and types of gene duplications, differences in duplication rates and sizes across chromosomes, and describe evidence of secondary modification through deletions, which will influence the extent to which these variants can serve as a source of genetic novelty.

Genotyping and Quality Control

Divergently-oriented paired-end reads are effective indicators of tandem duplications (Cridland and Thornton 2010, Zichner et al. 2013, Mills et al. 2011, Tuzun et al. 2005). We have used paired-end read orientation (Figure 2) combined with increased coverage in genomic sequencing (Figure 3) to identify tandem duplications in population samples of *D. yakuba* and *D. simulans*. Divergently-oriented reads indicative of putative tandem duplications were clustered within a single strain, with three or more divergently-oriented read pairs within the strain required to define each tandem duplication (see Methods). Duplications were then clustered across strains with coordinates defined as the maximum span of divergent reads across all strains. The distribution of supporting read pairs is

highly skewed, with 3-4 supporting read pairs for many calls (Figure S1). To account for duplications which may be undetected, we additionally included variants that showed two-fold increases (Figure 3) in quantile normalized coverage (Figure S2-S3) and which are supported by one or more divergently-oriented read pairs were also identified as having duplications if the duplicate was present in a second strain, thereby correcting sample frequency estimates for false negatives (see Methods, Text S1). We retained only those tandem duplications which are not present in outgroup reference genomes of *D. melanogaster*, *D. erecta*, and *D. yakuba* or *D. simulans* as defined in a BLAST search (see Methods) suggesting recent origins.

Using divergently-oriented paired-end reads, we have identified 1,415 segregating tandem duplications across 20 sample strains of *D. yakuba*, in comparison to 975 segregating tandem duplications in 20 lines of *D. simulans*, with significantly more duplicates identified in *D. yakuba* than in *D. simulans* (one-sided *t*-test $t = -3.8126$, $df = 24.593$, $P = 0.0004089$). More variants are identified in *D. yakuba* in spite of higher coverage in *D. simulans* (Table S4), suggesting that the difference is likely to be biological rather than technical. In fact, the number of variants identified is only weakly correlated with coverage per strain (Figure 4) a product of sequencing to the saturation point of coverage (Table S9). Downsampling reads from *D. yakuba* CY17C, which was sequenced to 151X, we find that the portion of the genome covered with 3 or more reads (the detection limit of our assay) plateaus at roughly 45X (Table S9), though lower coverage data used in previous studies (Sudmant et al. 2010, Zichner et al. 2013, Mills et al. 2011, Alkan et al. 2009) will be far from this plateau. The tandem duplications identified across these sample strains cover 2.574% of the assayable genome of the X and 4 major autosomes in *D. yakuba* and 1.837% of the assayable genome of the X and 4 major autosomes in *D. simulans*. We are able to identify tandem duplications as small as 66 bp in *D. yakuba* and 78 bp in *D. simulans*.

We have successfully PCR amplified $\frac{23}{46}$ randomly chosen variants in *D. yakuba* and $\frac{35}{42}$ variants in *D. simulans*. The rate of PCR confirmation in *D. simulans* is not significantly different from previous studies of CNVs, but we observe significant differences between *D. yakuba* and all other confirmation rates (Table S10). In view of this disparity, combined with difficulties of PCR primer design for variants whose precise structures are unknown, we generated PacBio long molecule sequencing data for 4 strains of *D. yakuba* in order to more reliably estimate the false positive rate (Table S11). PacBio long molecule sequencing has recently been used to validate targeted duplications in human genome data (Huddleston et al. 2014). We extend this approach to genome-wide identification and validation of tandem duplications, and have generated PacBio reads for four different sample strains of *D. yakuba*. Across these four strains, we observe confirmation of 661 out of 688 mutations, for a maximum false-positive rate of 3.9% (Table S8), though some variants may be unconfirmed due to low clone coverage in a region. Hence, the duplicates identified with paired-end reads in high coverage genomic sequence data are extremely accurate and comparable to or better than previous methods or attempts to identify and validate duplicates using lower coverage genomic sequences or microarrays (Mills et al. 2011, Alkan et al. 2009, Cardoso-Moreira et al. 2011, Zichner et al. 2013, Sudmant et al. 2010). Split read mapping with short

Illumina reads performed poorly in comparison and failed to confirm 88.3% of variants, and breakpoint assembly was possible for less than 60% of variants in spite of high rates of confirmation with PacBio (See SI Text). Thus, requiring these criteria would exclude the majority of variant calls and would likely be biased against duplicates with formation facilitated by repetitive sequences. Where duplicate breakpoints contain repetitive or low complexity sequences, or where subsequent modification of alleles through deletion has altered surrounding sequence, PCRs are likely to fail, and we would suggest that confirmation using long molecule sequencing is far more reliable in the face of complex structures. Further description of genomic sequences, tandem duplications, and discussion of paired-end read performance in high coverage genomic sequencing data in comparison to other methods is available in Text S1.

Complex variation

We identified deletions that have occurred in duplicated alleles using long-spanning read pairs 600 bp or longer, corresponding approximately to the 99.9th percentile of fragment lengths in the reference genomes (Table S5). Out of 880 duplications ≥ 600 bp in length in *D. yakuba* which could be surveyed for deletions within duplications using long-spanning reads, 151 (17%) contain long spanning read pairs covering 50% or more of the duplicate sequence in one or more strain, indicative of subsequent deletion, multiple independent short-range dispersed duplications, or incomplete duplication (Figure 5). In *D. simulans*, $\frac{39}{486}$ (8%) duplications ≥ 600 bp contain long-spanning reads covering 50% or more of duplicated sequence in one or more strains. Among 69 such modified variants in *D. yakuba* that are present in multiple strains, 66 have at least one strain that lacks these long-spanning reads, whereas 12 out of 14 variants in *D. simulans* lack long spanning reads in one or more strains. Given large numbers of unaltered duplicates the most parsimonious explanation is that deletions are most often secondary modification and that the majority of these constructs form through full length duplication and subsequent deletion rather than independent dispersed duplications.

In one well-characterized example, we have identified a duplication which spans the chimeric retrogene *jingwei* (*jgw*) (Long and Langley 1993), which houses a deletion upstream from *jgw* (Figure 6). The duplication is defined by 10 divergent read pairs and confirmed by split read mapping in PacBio long molecule sequencing, whereas the deletion is supported by 20 long-spanning read pairs in line NY66-2 and gapped alignment in PacBio reads (Figure 6). The same duplication and deletion are independently confirmed with PacBio sequences in line CY21B3. The duplication spanning *jgw* is found at a frequency of $\frac{5}{20}$ strains, while the deletion shown is observed only in CY21B3 and NY66-2, suggesting that the deletions is a secondary modification. A second independent duplication spans *jgw* in $\frac{4}{20}$ strains and is confirmed in PacBio data, indicating that the region has been modified multiple times in different strains.

Deletions are exceptionally common in *Drosophila* (Petrov, Lozovskaya and Hartl 1996), and several genetic mechanisms might offer means of excision in a short time frame after duplication. The large loop mismatch repair system can facilitate deletions of duplicated sequence to modify duplicated sequence as long as variants are polymorphic. The presence

of unpaired duplicated DNA during meiosis or mitosis would commonly invoke the action of the large loop mismatch repair system, which if resolved imprecisely, could result in the construct observed (Figure 7). Deletions lying within a duplication have a median size of 3.6 kb in *D. yakuba* and 1.8 kb in *D. simulans*. Such large deletions are well outside the norm for genome wide large deletions in mutation accumulation lines of *D. melanogaster*, which show an average 409 bp and maximum of 2.6 kb (Schridder et al. 2013). Deletions of this size however are consistent with the size of excised fragments in large loop mismatch repair of several kilobases (Kearney et al. 2001). Deletion during non-homologous end joining or homology mediated replication slippage might produce deletions as well though it is unclear whether mutation rates are naturally high enough to operate in short time frames. Thus, we would expect modification of duplicated alleles to be extremely common, especially in deletion-biased *Drosophila*.

Differences in gene duplications across species

Duplicated coding sequences can diverge to produce novel peptides, novel regulatory profiles, or specialized subfunctions (Conant and Wolfe 2008). In order to determine the extent to which genes are likely to be duplicated and whether particular categories of gene duplications are more likely to be favored, we identified coding sequences captured by tandem duplications. We find large numbers of segregating gene duplications in both *D. yakuba* and *D. simulans* including hundreds of whole gene duplications (Table 1). We used the maximum span of divergently-oriented reads across all strains to identify tandem duplications that capture gene sequences in *D. yakuba* or *D. simulans* and to determine their propensity to capture whole and partial gene sequences.

We find that 47.3% of tandem duplications in *D. yakuba* and 40.8% in *D. simulans* capture coding sequences. The average duplicated gene in *D. yakuba* covers 45.9% of the gene sequence and 60.5% of the gene sequence in *D. simulans*. There are 670 duplications that capture gene sequences, spanning 845 different genes in *D. yakuba*, while 398 duplications span 478 genes in *D. simulans*. Some 103 genes in *D. yakuba* and 65 genes in *D. simulans* are captured in multiple independent duplications, with some genes falling in as many as 6 independent putative duplications as defined by divergently-oriented reads in *D. yakuba* and 32 independent putative duplications in *D. simulans*. Such high rate of independent duplications in *D. simulans* is consistent with previous studies using microarrays (Cardoso-Moreira, Arguello and Clark 2012). In total 993 gene fragments in *D. yakuba* and 758 gene fragments in *D. simulans* exist as segregating copy number variants in the population, and 56 genes are duplicated in both species.

Assuming that unmodified duplications without deletions represent the original mutated state, in *D. yakuba*, $\frac{274}{845}$ (27.6%) of duplicated gene fragments span more than 80% of gene sequence and capture the translation start site while 65 (7.7%) capture 20% or less and the translation start site. In *D. simulans* $\frac{317}{478}$ (66.3%) duplicated gene sequences capture 80% or more of the gene sequence and the translation start, and 34 (7.1%) capture 20% or less and include the translation start. Based on a resampling of gene duplications in *D. yakuba*, *D. simulans* houses an overabundance of whole or nearly whole gene duplications ($P < 10^{-7}$)

and an underrepresentation of small fragments ($P = 0.00291$), suggesting differences in the occurrence of whole gene duplications across species due either to mutational pressures or selection.

Duplicate genes and rapidly evolving phenotypes

Biases in the rates at which duplications form in different genomic regions or a greater propensity for selection to favor duplications in specific functional classes can result in a bias in gene ontology categories among duplicated genes. We used DAVID gene ontology analysis software to identify overrepresented functions among duplicate genes in *D. yakuba* and *D. simulans*. In *D. yakuba* we observe 678 duplicated genes with orthologs in *D. melanogaster*. Overrepresented functional categories include immunoglobulins, extracellular matrix, chitins and aminoglycans, immune response and wound healing, drug and hormone metabolism, chorion development, chemosensory response and development and morphogenesis (Table S13). In *D. simulans* we observe 478 duplicated genes with orthologs in *D. melanogaster*. Overrepresented gene ontology categories include cytochromes and oxidoreductases plus toxin metabolism, immune response to microbes, phospholipid metabolism, chemosensory processing, carboxylesterases, glutathion transferase and drug metabolism, and sarcomeres (Table S13). In *D. simulans* 65 genes were involved in multiple independent duplications that have distinct breakpoints. Overrepresented gene ontology categories include immune response to bacteria, chorion development and oogenesis, chemosensory perception, and organic cation membrane transport (Table S14). In *D. yakuba* among 72 genes duplicated independently, chorion development and oogenesis, cell signaling, immune response, sensory processing, and development are overrepresented (Table S14).

There are 25 high frequency variants found at a sample frequency of $\frac{17}{20}$ or greater in *D. simulans*, including lipases and endopeptidases expressed in male accessory glands and several genes involved in immune response to microbes (Table S15). One gene arose independently and has reached high frequency twice in *D. simulans*. In *D. yakuba*, we observe 13 high frequency variants, including endopeptidases and AMP dependent ligases (Table S15). Both male reproductive proteins (Wong and Wolfner 2012) and immune response to pathogens (Lazarro and Clark 2012) are known for their rapid evolution, and therefore these genes are strong candidates to search for evidence of ongoing selective sweeps. Though mutational biases can produce similarities in gene ontology categories, the overabundance of toxin metabolism genes and immune response peptides in both species as well as the overrepresentation of chemoreceptors, chitin cuticle genes, and oogenesis factors suggests that duplications are likely key players in rapidly evolving systems.

Chimeric Genes and Altered Coding Sequences

If only one boundary of a tandem duplication falls within a coding sequence and thereby copies the 5' end of a gene, the resulting construct will recruit formerly non-coding sequence to form the 3' end of the coding sequence (Figure 8A). We observe 143 cases of recruitment of non-coding sequence in *D. yakuba* (Table S16-S17) and 96 cases in *D. simulans*

(Table S18-S19). Several of these are found at moderate frequencies greater than 50%. Overrepresented GO categories among genes in *D. simulans* include immune defense and sarcomeres, whereas genes with recruited sequence in *D. yakuba* show an overrepresentation of genes involved in locomotory behavior. We observe one high frequency variant in *D. yakuba* at a sample frequency of $\frac{17}{20}$, an Adenylate cyclase involved in locomotor rhythm as well as two high frequency variants in *D. simulans* LysB, an antimicrobial humoral response gene and a gene of unknown function. These high frequency chimeras are strong candidates for selective sweeps.

If both boundaries fall within different coding sequences, tandem duplications can create chimeric genes (Figure 8B) (Rogers, Bedford and Hartl 2009). We find 130 tandem duplications in *D. yakuba*, and 76 in *D. simulans* where both breakpoints fall within non-overlapping coding sequences. Some 11 of the 130 duplications in *D. yakuba* and 30 of 76 in *D. simulans* with both breakpoints in gene sequences face one another and as such are not expected to create new open reading frames, as the constructs will lack promoters. Another 40 of the 130 duplications in *D. yakuba* and 8 of 76 in *D. simulans* with both breakpoints in gene sequences, and will have promoters that can potentially transcribe sequences from both strands of DNA (Figure 9, Table S20-S21). Only 78 chimeric coding sequences in *D. yakuba* (Table S22-S23) and 38 chimeric genes in *D. simulans* (Table S24) have parental genes in parallel orientation. Among the parental genes of these chimeras, cytochromes and genes involved in drug metabolism are overrepresented in *D. yakuba*. Other functional categories which are present but not overrepresented include endopeptidases, signaling glycopeptides, and sensory signal transduction peptides. Among parental genes in *D. simulans*, Cytochromes and insecticide metabolism genes, sensory perception genes, and endopeptidase genes are overrepresented. Additional categories present include signal peptides, endocytosis genes, and oogenesis genes. Several such constructs are found at moderate frequencies above 10/20, suggesting that they are at least not detrimental. However, two chimeras in *D. yakuba* are found at high frequency. One formed from a combination of *GE12441* and *GE12442* is at a frequency of 16/20, and one formed from *GE12353* and *GE12354* is at a frequency of 19/20. In *D. simulans* one chimera, formed from *CG11598* and *CG11608*, is at a frequency of 20/20. All of these genes are lipases or endopeptidases. These high frequency variants are strong candidates for selective sweeps.

Compared to the number of tandem duplications that capture coding sequences, the number of duplications which form chimeric genes indicates that chimeric constructs derived from parental genes in parallel orientation form as a result of 10.4% of tandem duplications that capture genes in *D. yakuba* and 9.5% of tandem duplications that capture coding sequences in *D. simulans*. These numbers are in general agreement with rates of chimeric genes formation estimated from a within-genome study of *D. melanogaster* of 16.0% compared to the rate of formation of duplicate genes (Rogers, Bedford and Hartl 2009).

Association with transposable elements and direct repeats

Repetitive sequences are known to facilitate ectopic recombination events that commonly yield tandem duplications (Lim and Simmons 1994). In *D. yakuba*, 179 (12.7%) tandem

duplications fall within 1 kb of a TE in at least one sample strain that has a duplication and 52 (3.7%) fall within 100 bp of a TE (Table S25). In *D. simulans*, 122 (12.5%) lie within 1 kb of a TE and 53 (5.4%) fall within 100 bp of a TE (Table S25). Additionally, 125 (8.8%) of duplications in *D. yakuba* have 100 bp or more of direct repeated sequence in the 500 bp up and downstream of duplication boundaries and 237 (16.7%) have 30 bp or more in the reference sequence as identified in a BLASTn comparison of regions flanking divergently-oriented read spans at an E-value $\leq 10^{-5}$ (Table S25). In *D. simulans*, 56 (5.7%) have 100 bp or more of direct repeated sequence in the 500 bp up and downstream of duplication boundaries in the reference and 150 (14.4%) have 30 bp or more of repeated sequence (Table S25). In total 371 duplications in *D. yakuba* and 243 duplications in *D. simulans* either lie within 1 kb of a transposable element in at least one strain or are flanked by 30 bp or more of direct repeated sequence. Hence, a maximum of 26.2% of duplications identified in *D. yakuba* and 24.9% of duplications identified in *D. simulans* may have been facilitated by ectopic recombination between large repeats, consistent with previous estimates from single genome studies of 30% in *D. melanogaster* but somewhat higher than those in *D. yakuba* of 12% (Zhou et al. 2008).

In *D. yakuba*, 14.4% of duplications with 100 bp or more of repetitive sequence and 21.1% of duplications with 30 bp or more are located on the X. In contrast, 46.4% of duplications in *D. simulans* with 100 bp or more of direct repeated sequence in the reference and 44.7% with more than 30 bp of repeated sequence in the *D. simulans* reference lie on the X chromosome. Based on a resampling of randomly chosen duplications, duplications on the X chromosome are overrepresented among duplications with direct repeats ($P < 10^{-7}$) but the same is not true of duplicates with direct repeats in *D. yakuba* ($P = 0.248$). A genome wide blastn comparison shows that direct repeats are not overrepresented on the *D. simulans* X chromosome and cannot explain the observed association (Table S26) Hence, duplication via ectopic recombination may be exceptionally common on the X chromosome in *D. simulans*.

Excess of duplications on the *D. simulans* X

The distribution of duplication sizes was calculated for each major chromosomal arm in each species. Average duplicate size is 2,518 bp, in close agreement with that observed in mutation accumulation lines in *D. melanogaster* (Schridder et al. 2013) but somewhat larger than that observed using microarrays in *D. simulans* (Cardoso-Moreira et al. 2011). The X chromosome in *D. yakuba* displays an overabundance of small duplications in comparison to each of the autosomes in a Tukey’s HSD test after correction for multiple testing with 27% of duplicates 500 bp or less ($P \leq 6.8 \times 10^{-5}$, Figure 1, Figure 10A, Table S27). Chromosome 2R is also significantly different from the other three major autosomal arms ($P \leq 2.95 \times 10^{-3}$, Figure 10A, Table S27). However, in *D. simulans* there is no significant difference between the X and 2R, 2L and 3R, even though the X houses a greater density of duplications (Figure 10B). The *D. simulans* chromosome 3L is different from 2L ($P = 0.029$, Figure 10B, Table S27).

We observe a significant effect in the number of duplications per mapped base pair

by chromosome in both *D. yakuba* ($F(5, 109) = 8.321$, $P = 1.09 \times 10^6$) and *D. simulans* ($F(5, 113) = 36.74$, $P < 2 \times 10^{-16}$). In a post-hoc Tukey’s HSD test with correction for multiple testing, the *D. simulans* X chromosome contains more duplications per mapped base pair than any of the autosomes, with 316 duplications ($P \leq 1.0537 \times 10^{-4}$, Table S28, Figure 1, Figure 11). Chromosome 2R contains an excess of duplicates in comparison to chromosome 3R ($P = 0.032$), but all other pairwise comparisons of the four major autosomes are not significant. Chromosome 4 contains an excess of duplications per mapped base pair in comparison to all other chromosomes in both *D. simulans* and *D. yakuba*. In *D. yakuba* the X is different from 3L ($P = 0.039$) but not from any other autosome. Some 11 of the 25 duplicates in *D. simulans* are at a frequency of $\frac{17}{20}$ strains or greater (44%) on the X (Figure 1). In comparison, only 2 of the 13 high frequency duplications in *D. yakuba* (15.4%) are located on the X, nor do we see a comparable overabundance of duplications on the *D. yakuba* X. These results point to a clear excess of duplications on the X chromosome in *D. simulans* in comparison to the autosomes, as well as an overabundance of duplications on the fourth chromosome in both species.

Given the excess of duplications associated with repetitive content on the *D. simulans* X, repetitive elements may be an important factor in forming the observed overabundance of duplications on the *D. simulans* X. While mutational and selective processes can lead to a bias in the number of duplications that form on different chromosomes, the excess of high frequency variants on the *D. simulans* X at a frequency of 20 out of 20 would suggest that at least some of the overabundance on the *D. simulans* X is due to selective forces or demography resulting in duplicates spreading through the population.

Discussion

We have used paired-end reads to describe tandem duplications in sample strains of *D. yakuba* and *D. simulans*, their sample frequencies, and the genes that they affect. We use high coverage Illumina genomic sequencing data of 50X or greater to successfully identify tandem duplications among individually sequenced isofemale lines derived from natural populations. We have filtered tandem duplications to include recently-derived segregating tandem duplicates that are not present in the reference genome of each species for genomic regions that have coverage of three or more read pairs across all sequenced strains. We show high rates of confirmation using long molecule PacBio sequences with 96.1% of variants showing evidence of confirmation.

We identify 1415 tandem duplicates in *D. yakuba* and 975 in *D. simulans*, indicating that there is substantial standing variation segregating in populations that may contribute adaptive evolution and the instance of detrimental phenotypes. We identify hundreds of chimeric genes and cases where genes recruit formerly non-coding sequence. We have shown an excess of duplications on the *D. simulans* X chromosome as well as an overabundance of whole gene duplications in *D. simulans*, suggestive of selection acting on duplications.

Rapid modification of duplicated alleles

Standing variation is expected to play a major role in adaptation and evolutionary change (Barrett and Schluter 2008). If the span of standing variation in populations is limited, the dynamics, genomic content, and variability of standing variation in populations is likely to play a defining role in evolutionary outcomes. The observed span of tandem duplications across strains is limited, with 2.574% of the assayable genome of the X and 4 major autosomes in *D. yakuba* and 1.837% of the assayable genome of the X and 4 major autosomes in *D. simulans*. Yet, the variation that is observed portrays a dynamic picture of gains and losses with evidence that duplications can induce subsequent deletions through large loop mismatch repair, suggesting that regions that are duplicated create genomic instability. The resulting expansion and contraction of genomic sequences will contribute to greater variability in these limited regions than has been suggested to date, offering wider variation upon which selection can act. Up to 17% of duplications in *D. yakuba* and 8% of duplications in *D. simulans* show long spanning reads in one or more strains, indicative of complex changes such as subsequent deletion, insertion of foreign sequence, or incomplete or short-range dispersed duplication (Figure 5). These results are consistent with complex breakpoints previously observed in *D. melanogaster* (Cridland and Thornton 2010). Moreover, coverage changes for certain variants are consistent with duplication followed by subsequent deletion in one or both copies (Figure S4). Hence, the current pool of genetic diversity will in fact be far greater than simple interpretation of divergently-oriented reads or split read mapping might indicate. The majority of such changes have one or more strains with no signs of modification, suggesting that these variants are primarily duplications followed by deletions.

Secondary deletions of recently duplicated alleles may be exceptionally common, especially in deletion-biased genomes like *Drosophila*. Deletion of excess unpaired DNA for polymorphic duplicates during large loop mismatch repair, excision of transposable elements, replication slippage, and deletion during non-homologous end joining all offer common mechanisms that are likely to remove portions of duplicated alleles. Among these mechanisms, the large loop mismatch repair system specifically targets newly added DNA and is likely to be a driving force in the rapid modification of duplicated alleles. In the ideal case, precise excision would simply return the construct to singleton state resulting in a rapid cycle of mutations and reversions. However, when such removal is imprecise, these subsequent deletions are likely to modify duplicated sequences leaving incompletely duplicated segments. The average distance spanned by these putative deletions is over 2 kb, well above the mean for deletions observed in mutation accumulation lines of *D. melanogaster* (Schridder et al. 2013), but in agreement with the amount of DNA that can be efficiently removed by large loop mismatch repair (Kearney et al. 2001).

Duplications have the potential to induce secondary deletions quickly, while variants remain polymorphic, thereby offering mechanisms for rapid and potentially drastic genomic change that can potentially alter gene content, dosage, and regulation. Variation in populations, while limited in its genomic scope, may offer multiple variant forms at individual duplication sites. Thus, the substrate that is present for selection and adaptation will be far richer than a simple duplication or single copy, but rather can take on these complex forms of

modified variants that remain largely unexplored in terms of their molecular and evolutionary impacts. Thus, although the observed amount of variation is limited to only a fraction of the genome, the level of variation at these duplicated sites portrays an exceptionally dynamic flux of duplications and deletions at these sites that will result in changes in the content and organization of the genome and therefore is expected to have a strong influence on evolutionary outcomes.

D. yakuba displays 1.5 times as many duplications in comparison to *D. simulans*, as well as a two-fold enrichment in the percentage of variants with signals of deletion in one or more copy and higher population level mutation rates. The rapid flux of duplication and deletion observed in *D. yakuba* has produced a wider array of standing variation, which is expected to have a significant effect on evolutionary trajectories. *D. yakuba* will likely display a greater tendency toward pathogenic phenotypes associated with tandem duplicates (Emerson et al. 2008, Hu and Worton 1992) but also a greater source of standing variation that can be useful in adaptation and the development of novel traits (Conant and Wolfe 2008). Estimates of N_e in *D. yakuba* are higher than in *D. simulans*. We would thus expect greater instances of detrimental duplicates to be higher in *D. simulans* than in *D. yakuba*, but neutral mutations will collect more quickly across populations of *D. yakuba* due to high N_e . Hence, we suggest that the overabundance of duplicates in *D. yakuba* is not due to drift. Neither do we observe an excess of high frequency variants in *D. yakuba* that might be suggestive of selection, especially with respect to polymorphic variants.

Based on birth-death models of gene families, *D. simulans* is suggested to have high rates of duplication, whereas *D. yakuba* showed only moderate rates of gene family evolution (Hahn, Han and Han 2007). This may in fact be influenced by the overabundance of whole gene duplicates in *D. simulans* and not a reflection of genome wide mutation rates. The dichotomy between reference genomes and genome wide polymorphic variants might putatively be driven by selection for whole gene duplicates in *D. simulans* or mutational biases toward whole gene duplications.

Chimeric genes

Chimeric genes are a known source of genetic novelty that are more likely to produce regulatory changes, alterations in cellular targeting and membrane bound domains, as well as selective sweeps in comparison to whole gene duplications (Rogers and Hartl 2012). Chimeric genes have been known to produce peptides with novel functions in *Drosophila* (Long and Langley 1993, Zhang et al. 2004, Ranz et al. 2003) and in humans (Zhang et al. 2009, Ohshima and Igarashi 2010) and many are associated with adaptive bursts of amino acid substitutions (Jones and Begun 2005, Jones, Custer and Begun 2005). We observe large numbers of recently-derived chimeric constructs within populations, with 222 chimeric genes or genes that recruit non-coding sequence in *D. yakuba* and 134 in *D. simulans*, even in a limited sample of 20 strains per species.

In spite of their known role in adaptation, the majority of copy number variants are thought to be detrimental (Emerson et al. 2008, Cardoso-Moreira et al. 2011, Hu and Worton 1992). Chimeric genes are associated with human cancers, and the molecular changes

associated with chimera formation may contribute to their role as causative factors in human disease. The molecular changes that are facilitated by chimera formation (Rogers and Hartl 2012) likely contribute to their detrimental impacts on organisms and their role in disease as well as their potential for adaptation. We observe large numbers of chimeric genes that are identified as single variants in the population. Thus, chimeras may play the dual role of key players in adaptation to novel environments and as agents of detrimental phenotypic changes. The large amounts of standing variation observed may therefore contribute to disease alleles in populations, and proper identification is likely to be important for studies in human health.

Breakpoint determination

Many variants have breakpoints that cannot be assembled *de novo* from Illumina sequences (Table S30). Yet, we observe a 96.1% confirmation rate using PacBio reads. These results imply that breakpoints are often repetitive, low-complexity sequence or contain novel insertions and secondary events that are difficult to determine from paired-end read mapping alone or current naive *de novo* assembly methods. Hence, although paired-end Illumina read mapping is highly accurate, it cannot ascertain breakpoints to single base pair resolution in the majority of cases. Moreover, requiring breakpoint assembly to identify duplications will produce a strong ascertainment bias against up to 50% of all variants. This bias is more severe for small variants, even in *Drosophila*, which have compact genomes and few repeats in comparison to plants or vertebrates. Thus, short high-throughput Illumina reads orientation mapping offers an accurate but incomplete picture of variation present in the population, which can now be clarified with low coverage long read sequencing data.

Microarrays and coverage are subject to affects of mis-probing, mis-mapping, and large amounts of noise relative to signal (Figure S4). However, where accurate, arrays may reflect the span of duplicated segments more accurately than divergent reads alone, as they would accurately reflect deletion after duplication. However, the presence of complex events such as subsequent deletions may, if not properly identified and accounted for, overestimate of the mutation rate of duplications and underestimate their frequency in the population by claiming a modified variant as an independent duplication. Here, the directional nature and spatial relationships of read pair mapping shows advantages: divergently-oriented reads distinguish duplication whereas long spanning properly oriented reads can indicate a deletion with greater clarity and properly identify subsequent modification. Identifying putative deletions in duplicated sequences requires a tight distribution of insert sizes during library preparation (Table S5) but offers a far more complete picture of variation that is segregating in populations and more accurate estimation of variant frequencies that is well worth the effort.

The X chromosome

The *D. simulans* X chromosome appears to be unusual in that it contains an excess of duplications per mapped base pair in comparison to the autosomes, and an overabundance

of duplications associated with long repeats. Within-genome surveys of non-synonymous mutations in the *D. simulans* reference (Andolfatto, Wong and Bachtrog 2011) and large numbers of high frequency derived variants among non-synonymous sites and UTRs in *D. simulans* (Haddrill, Bachtrog and Andolfatto 2008) indicate widespread selective sweeps acting on the X chromosome. Similarly, we identify an excess of variants identified at high frequency on the *D. simulans* X, consistent with previous work using microarrays (Cardoso-Moreira et al. 2011). In *D. melanogaster*, the X chromosome contains greater repetitive content (Mackay et al. 2012), displays different gene density (Adams et al 2000), has potentially smaller population sizes (Wright 1931, Andolfatto 2001), lower levels of background selection (Charlesworth 2012), and an excess of genes involved in female-specific expression (Ranz et al. 2003) in comparison to the autosomes. Moreover, X chromosomes are subject to selfish genetic elements and often play a role in speciation (Presgraves 2008). Thus, the X chromosome may be exceptionally subject to widespread selection, and the role of tandem duplicates as responders to selective pressures deserves future exploration.

Similar patterns of high frequency variation have not been observed in *D. yakuba*, suggesting that evolution proceeds differently across the different species. The *D. yakuba* X chromosome has an excess of small duplications, which might potentially indicate selection acting against large duplications on the *D. yakuba* X. Tandem duplications are known to be detrimental, and given the hemizygous state of the X chromosome in males, we would expect purifying selection to act quickly on the X. The extent to which these patterns observed in *D. yakuba* may be driven by selection or demography remains to be seen, and is an important open question deserving of future study.

Methodological approach

Originally, high throughput detection of copy number variation relied on microarrays or SNP chips available at the time (Emerson et al. 2008, Dopman and Hartl 2007, Ionita-Laza et al. 2009, Conrad et al. 2010), and therefore suffers from problems of mis-probing, variable hybridization intensities, and dye effects, producing large amounts of noise relative to signal (Ionita-Laza et al. 2009). More recent studies have focused solely on changes in Illumina or 454 coverage analogous to changes in hybridization intensity (Sudmant et al. 2010). We have used coverage changes in combination with divergently oriented reads to identify variants using comparisons to a resequenced reference and quantile normalized coverage data to correct for stochastic coverage changes, repetitive content, GC bias and low complexity sequence, resulting in robust variant calls. Furthermore, the common practice of retaining only variants that are present in multiple samples or at particular genotype frequencies (Conrad et al. 2010), detected by multiple independent methods (Mills et al. 2011, Zichner et al. 2013, Alkan et al. 2009), or that are larger than several kilobases (Alkan et al. 2009, Xie and Tammi 2009, Sudmant et al. 2010) can lead to severe ascertainment bias both with respect to the types of variants that are present, the estimation of their prevalence within populations and contribution to disease phenotypes, and the evolutionary impacts of duplicated sequences.

With more recent improvements in Illumina sequencing technology, we have been able

to sequence strains individually to 50X or greater coverage. The use of paired-end reads in extremely high coverage data provides clear advantages over previous work using roughly 3.6X-25X with subsets sequenced to 30-42X (Sudmant et al. 2010, Zichner et al. 2013, Mills et al. 2011), or 16X (Alkan et al. 2009). The high coverage data presented here covers the majority of the assayable genome and we exclude only a few percent of variant calls due to low coverage across strains (Table S9). Thus, we are able to identify hundreds of events that have 3 or more supporting divergent read pairs that might be missed at lower coverage (Figure S1). We have additionally filtered sequences to exclude ancestral duplications, similarly to previous work in humans (Mills et al. 2011) allowing for identification of derived mutations. The result is a high confidence dataset for recently-derived tandem duplications in data that effectively surveys the majority of the assayable genome. This high coverage is essential in ensuring valid results from the sole use of paired-end read orientation. However, the types of duplications that can be detected is highly dependent on sequencing library insert size. For breakpoints with large amounts of repetitive sequence, reads separated by 300 bp may not be sufficient to overcome difficulties of read mapping. Additionally, the minimum duplication size is also limited by insert size. Capturing these types of constructs using paired-end reads, especially in organisms with large amounts of repetitive content, including nested transposable elements, will require a more diverse range of library insert sizes, a factor that is likely to be important for surveys of larger, more repetitive genomes.

We are able to identify copy number variants as small as 66 bp using divergently-oriented paired-end reads, even in cases where nucleotide divergence between paralogs or partially repetitive sequence might otherwise complicate their discovery through coverage changes or split read mapping using short reads. Divergently-oriented reads are additionally reliable to detect duplications in regions where distributions of coverage are too irregular to allow for automated detection of duplicates. We observe a high 96.1% confirmation rate of variants among four sample strains of *D. yakuba* using PacBio reads up to 24 kb in length, suggesting that paired-end reads in high coverage genomic sequencing will grossly outperform previous methods which show high false positive and false negative rates. Moreover, the use of the newly annotated *D. simulans* genome (Hu et al. 2012) based on a single isofemale line will result in improved accuracy in comparison to previous studies in *D. simulans* (Cardoso-Moreira et al. 2011). The general principles of the paired-end approach should be broadly applicable and similar methods already have been used to identify chromosomal inversions in natural populations (Corbett-Detig, Cardeno and Langley 2012). PacBio reads can confirm structural variants with high rates of success, even given low coverage and nucleotide high error rates (Huddleston et al. 2014) and we have extended this approach to our genome wide survey. However, the ambiguity of split read mapping in the face of repetitive elements can still complicate *de novo* duplicate discovery using split read mapping of long reads. Furthermore, for the present, generating high coverage genomic sequencing equivalent to that of our paired-end Illumina data is not cost-effective. However, this technology and similar long read approaches are likely to offer advantages in confirming or discovering structural variants such as tandem duplications, as well as *de novo* assembly, that is worth future exploration.

We are able to identify and confirm a large number of complex gene structures such as chimeric genes, recruitment of adjacent non-coding sequence, potential coding sequence disruption, and potential selective silencing of expression. These complex mutations are often associated with cancer and other diseases (Ionita-Laza et al. 2009, Inaki and Liu 2012) and are most likely to cause pathogenic outcomes. Hence the methods described here will be broadly applicable in GWAS and clinical studies as well as in evolutionary genetics of non-model systems where next generation sequencing has so recently made population genomics readily tractable.

Conclusions

Here, we have described the landscape of standing variation for tandem duplications in isofemale lines derived from natural populations of *D. yakuba* and *D. simulans* with high accuracy. The resulting portrait of hundreds to thousands of variants, including large numbers of complex breakpoints, modifying deletions, cases of recruited non-coding sequence, and dozens of chimeric genes per species reveals a rich substrate of segregating variation across populations. We show that although the span of duplications across the genome is quite limited, duplicates can induce secondary mutations and result in dynamic changes, resulting in greater variation across mutated sites that offers more abundant variation for use in adaptation than has been previously portrayed. The ways in which this variation influences adaptive evolution and produces molecular changes will clarify the extent to which mutational profiles define evolutionary outcomes and the ways in which molecular changes associated with tandem duplications serve as causative factors in disease.

Materials and Methods

Population Samples

We surveyed variation in 10 lines of *D. yakuba* from Nairobi, Kenya and 10 from Nguti, Cameroon (collected by P. Andolfatto 2002) as well as 10 lines of *D. simulans* from Madagascar (collected by B. Ballard in 2002) and 10 strains from Nairobi, Kenya (collected by P. Andolfatto in 2006). Flies from these isofemale lines (i.e. descendants from a single wild-caught female) were inbred in the lab for 9-12 generations of sibling mating. These should provide effectively haploid samples of allelic variation representative of natural populations.

In addition to the 20 inbred lines derived from wild-caught flies, we also sequenced the reference strains for each species. For *D. simulans*, the reference strain is the w^{501} stock (UCSD stock center 14021-0251.011), whose sequence is described in (Hu et al. 2012). For *D. yakuba*, the reference strain is UCSD stock center 14021-0261.01, and the genome sequence is previously described in (Drosophila Twelve Genomes Consortium 2007). The majority of the wild-caught strains and the *D. yakuba* reference stock were sequenced with three lanes of paired-end sequencing at the UC Irvine Genomics High Throughput Facility (<http://>

dmaf.biochem.uci.edu). The sequencing of the *D. simulans* reference strain was described in (Hu et al. 2012). The number of lanes and read lengths per lane are summarized in Tables S2 and S1.

Alignment to reference

The sequencing reads were aligned to the appropriate reference genome (Drosophila Twelve Genomes Consortium 2007, Hu et al. 2012) using `bwa` version 0.5.9 (Li and Durbin 2009) with the following parameters, `bwa aln -l 13 -m 50000000 -R 5000`. The resulting paired-end mappings were resolved via the “sampe” module of `bwa` (`bwa sampe -a 5000 -N 5000 -n 500`), and the output was sorted and converted into a “bam” file using `samtools` version 0.1.18 (Li et al. 2009). In the alignment and resolution commands, `-l` is the hash sized used for seeding alignments, and the `-R`, `-a`, `-N` and `-n` refer to how many alignments are recorded for reads mapping to multiple locations in the reference. After the paired-end mapping resolution, the bam files from each lane of sequencing were merged into a single bam file sorted according to position along the reference genome. A second bam file, sorted by read name, was then created for use as input into our clustering software.

Clustering abnormal mapping events

Tandem duplications should be readily apparent among mapped reads as sequenced read pairs that map in divergent orientations (Cridland and Thornton 2010, Zichner et al. 2013, Mills et al. 2011, Tuzun et al. 2005), provided that tandem duplications with respect to a reference genome result in a single novel junction. Figure 2 shows a putative genomic sample that contains a tandem duplication of a gene that was used to generate paired-end sequencing reads. We allowed for up to two mismatches within mapped reads in order to capture divergent read calls in sample strains that have moderate numbers of nucleotide differences. Reads were required to map uniquely, and so if duplication breakpoints contain entirely repetitive sequences with no divergence across copies in the genome, they will not be found. These limitations will, however, have minimal effects (see Text S1).

Sets of read pairs in the same strain that are located within the 99.9th quantile of the mapping distance between properly mapped pairs from one another were clustered together into a single duplication. In practice, this threshold distance is roughly 1 kb. Tandem duplications were identified as regions where 3 or more divergently-oriented read pairs cluster to the same location in a single strain. Allowing fewer divergent reads leads to a large number of false positive duplication calls due to cloning and sequencing errors. Further detail is offered in Text S1.

PacBio alignment and analysis

FASTQ files of PacBio reads were aligned to the *D. yakuba* reference (Drosophila Twelve Genomes Consortium 2007) using `blasr` (Chaisson and Tesler 2012), available from <https://github.com/PacificBiosciences/blasr>, with default options and storing the resulting

alignments in a bam file. Alignments from regions within 1 kb of putative tandem duplications called using short read data (divergent read orientation plus an increase in coverage) were extracted from the bam files using `samtools` 0.1.18 (Li et al. 2009). Reads falling within these regions were then pulled and realigned to the reference using a BLASTn (Altschul et al. 1990) with low-complexity filters turned off (-F F) at an *E*-value cutoff of 0.1 to allow for short alignments given the high error rate of PacBio sequencing. Alignment using `blastn` proved important because it revealed cases where the bam files resulting from `blsr` alignments failed to record secondary hits for a read, especially in cases where alignments are on the order of hundreds of base pairs. Here, confirmation benefits from long sequences which can anchor reads uniquely to a region, producing greater confidence in split-read alignments. Variants were considered confirmed if two segments of a single PacBio subread which do not overlap by more than 20% align to overlapping sections of the reference (Figure S5B) or if a single read aligns in split formation with the downstream end of the read aligning to an upstream region of the reference (Figure S5A,C-E). An event was considered not confirmed if there were no long reads showing any of the alignment patterns in Figure S5 within 1 kb of the variant. Variants were considered definite false positives if clearly contradicted by at least one read spanning the entire putatively duplicated region as defined by Illumina read mapping and adjacent reference. Some of these unconfirmed variants may be due to low clone coverage in the region or lack of sufficient read lengths rather than false positives.

HMM and coverage changes

To detect increases and decreases relative to reference resequencing, we quantile normalized coverage for each strain in R so that coverage displayed an equal median and variance across all strains (Bolstad et al. 2003). Such normalization renders tests of differing coverage robust in the face of differing sequence depth across samples or across sites and is essential for reliable confirmation of tandem duplicate calls (Bolstad et al. 2003).

We developed a Hidden Markov Model to identify statistically significant increases in coverage at duplicated sites. In the HMM, hidden states are defined by copy number and they act to effect differential emission probabilities for the observed outcomes of coverage depth at duplicated or non duplicated sites. We modeled differences in coverage for sample strains relative to the reference as the difference in two normal distributed random variables each with a mean and variance corresponding to the observed mean and variance in the reference in the given window. Detailed methods of the HMM and decoding are provided in Text S1.

Deletions and complex duplication events

In order to determine the extent to which secondary deletions, incomplete duplications, or short range dispersed duplicates result in complex structures that are not representative of classic duplications, we identified long-spanning read pairs that lie within tandem duplications. We identified read-pairs with an estimated template length of ≥ 600 bp, corresponding to roughly the 99.9th percentile of fragment lengths in the reference genome

(Table S5). Long spanning reads whose end points lie within 200 bp of one another and which are fully contained within the duplication endpoints were clustered together. Clusters supported by five or more read pairs (corresponding to a putative P -value of 10^{-15}) were recorded as signs of deletion or other complex rearrangement.

Sample frequency of variants

Complex mutations that are present in two different strains and have divergent reads spanning regions on both the 5' and 3' ends that fall within 100 bp of one another in the two strains are considered to be equivalent duplications. While divergently-oriented reads reliably identify duplications, the true boundaries of the duplication may differ from the divergent read spans by several bases, especially in cases where repetitive or low complexity sequence lies at breakpoints, a complication which is not addressed in recent work (Zichner et al. 2013, Mills et al. 2011). For each duplication the minimum of divergent read starts and the maximum of divergent read stops across all strains was recorded to indicate the span of the duplication. These breakpoints were assembled and confirmed *in silico* using phrap and lastz (Text S1).

In order to correct frequencies for the effects of false negatives, we used a combination of coverage and divergently-oriented reads to identify tandem duplicates in additional strains. For each duplication present based on three or more pairs divergent reads in at least one strain, a different strain which had at least one divergently-oriented read-pair and displayed two-fold or greater coverage increases as determined by the HMM across at least 75% of the duplication's span was also recorded as having that particular duplication as well.

We retained tandem duplicates with divergent read pairs where the minimum start and the maximum stop after clustering were less than 25 kb apart. While there may be some tandem duplications larger than 25 kb, divergent read pairs at a greater distance are substantially less likely to display two-fold coverage changes across the entire span and are therefore more consistent with translocations within chromosomes (Table S31). Unannotated duplications in the reference are likely to be biased towards specific sizes, GO classes, or genomic locations and are likely to artificially influence statistical tests. We removed duplications that were also identified in the reference, and did not include these in downstream analyses of duplication sizes or numbers, gene ontology, or site frequency spectra.

Polarizing ancestral state

All tandem duplications identified are polymorphic in populations and are therefore expected to be extremely young. However, tandem duplications may be identified in sample strains relative to the references if they are new mutations in the sample or if they represent ancestral sequence that has returned to single copy in the reference through deletion. In order to identify duplications that represent the ancestral state, we pulled reference sequence corresponding to the maximum duplicate span and ran a BLASTn comparison of

the sequence against the *D. melanogaster*, *D. erecta*, and *D. yakuba* or *D. simulans* reference genomes at an *E*-value cutoff of 10^{-5} .

Ancestral tandem duplications were defined as any segment that has two hits on the same chromosome of the given reference that lie within 200 kb of one another, excluding unlocalized sequence and heterochromatin annotations where assembly and annotations are uncertain. Ancestral duplications that are shared across species should be separated by moderate numbers of nucleotide differences, and therefore are expected to be correctly assembled across outgroups. Hits must have at least 85% nucleotide identity and must span at least 80% of the contig spanned by divergently-oriented reads in the sample. Based on these requirements, we removed 8.1% of duplications in *D. simulans* and 3.3% in *D. yakuba*, suggesting that the vast majority of duplicates identified are recently derived, as expected.

Transposable Element Annotation and Repetitive Content

Transposable elements were initially identified in the *D. simulans* and *D. yakuba* reference sequences by identifying all read pairs where one member of the pair aligned uniquely to the reference and the other member of the pair aligned multiply. This has been previously demonstrated to be an indication of a TE breakpoint (Mackay et al. 2012, Cridland et al. 2013) All locations to which these multiply aligning reads align were recorded and a fasta file of these putative TE locations was generated. Putative TE sequences were then aligned to the set of annotated TEs in version 5 of the *D. melanogaster* reference downloaded from flybase (www.flybase.org) using tblastx (Altschul et al. 1990) with the following parameters (-f 999 -F "" -e 10^{-4} -m 8). Regions of the reference sequence that aligned to a *D. melanogaster* TE with an E-value of $\leq 10^{-9}$ were kept and annotated as TEs. We then extracted 500 base pairs to either side of the annotated regions of the reference and aligned these regions to the set of *D. melanogaster* TEs, as above. This procedure was performed twice to capture the full length of TE sequence in the reference genomes.

Once transposable elements were annotated in the reference genomes, TEs were detected in the 20 sample genomes (Mackay et al. 2012) which includes both TE presence and TE absence calls. Briefly, initial TE detection was done by identifying all read pairs where one member of the pair aligned uniquely to the reference and the other member aligned to any known TE sequence were identified. Unique reads were clustered if they aligned to the same strand of the same chromosome, within a given threshold distance. This threshold was defined as the 99th quantile of mapping distances observed for uniquely mapping read pairs that are properly paired and lie in the expected orientation on opposite strands. At least three read pairs from each of the left and right estimates, in the correct orientation and correct strand, were required to indicate a TE. Phrap (version 1.090518) (Ewing and Green 1998) with the following parameters (-forcelevel 10 -minscore 10 -minmatch 10) was used to reassemble the local area around the TE insertion breakpoint. Contigs were classified according to TE family based on alignments in a BLASTn search (Altschul et al. 1990).

Following the initial TE detection phase we examined each position where a TE was identified, including TEs identified in the appropriate reference, in each other line in that

species. At this stage we were able to both identify TEs which had previously been missed by our pipeline as well as to make absence calls by reconstructing a contig that spans the TE insertion location. Repetitive content independent of transposable elements was defined using an all-by-all BLASTn comparison (Altschul et al. 1990) of sequence 500 bp upstream and downstream of duplication coordinates in the *D. yakuba* and *D. simulans* references at an E-value $\leq 10^{-5}$ with no filter for low complexity or repetitive sequences. We used a resampling approach to identify overrepresentation of duplications associated with direct repeats. We performed 10,000,000 replicates choosing the same number of tandem duplications at random and determining whether an equal or greater number were identified on the X chromosome.

Tandem repeats which might putatively facilitate ectopic recombination may hinder identification of tandem duplicates if repeat sequences are identical. We performed an all-by-all blastn of all chromosomes for each of the reference genomes at an E-value of 10^{-5} with low complexity filters turned off (-F F). Ignoring identical self hits, we identified all directly repeated sequences with greater than 99.5% nucleotide identity which are greater than 300 bp in length and which lie within 25 kb of one another, in accordance with the criteria for identifying duplicates.

Identifying duplicated coding sequence

Gene duplications were defined as any divergent read calls whose maximum span across all lines overlaps with the annotated CDS coordinates. *D. yakuba* CDS annotations were based on flybase release *D. yakuba* r.1.3. Gene annotations for the recent reassembly of the *D. simulans* reference were produced by aligning all *D. melanogaster* CDS sequences to the *D. simulans* reference in a tblastx. Percent coverage of the CDS was defined based on the portion of the corresponding genomic sequence from start to stop that was covered by the maximum span of divergent read calls across all strains.

Gene Ontology

We used DAVID gene ontology analysis software (<http://david.abcc.ncifcrf.gov/>, accessed Mar 2013) to determine whether any functional categories were overrepresented at duplicated genes. Functional data for *D. yakuba* and *D. simulans* are not readily available in many cases, and thus we identified functional classes in the *D. melanogaster* orthologs as classified in Flybase. Gene ontology clustering threshold was set to Low and significance was defined using a cutoff of EASE ≥ 1.0 . The DAVID clustering software uses Fuzzy Heuristic Partitioning to identify genes with related functional terms at all levels of Gene Ontology from cellular processes to known phenotypes.

Differences among chromosomes

We calculated the size of duplications that span less than 25 kb in each sample strain, excluding duplications identified in the reference, as incorrectly assembled duplicates are

likely be biased toward repetitive and low complexity sequence. Significant differences in duplication sizes were identified using ANOVA and Tukey's Honestly Significant Difference test on the log normalized distribution of duplication sizes by chromosome.

We calculated the number of duplications that span less than 25 kb on each major chromosomal arm for each sample strain, excluding duplications identified in the reference. The number of duplications was then normalized by the number of mapped bases in the reference to adjust for different chromosome sizes and coverage. Differences in the number of duplications per base pair were identified using ANOVA and Tukey's Honestly Significant Difference test. There was no significant difference in the number of duplications present across lines.

Supporting Files

Extended methods as well as detailed description of sequence data and confirmation is provided in Text S1. All data files are available at molpopogen.org/Data. Aligned bam files were deposited in the National Institutes of Health Short Read Archive under accession numbers SRP040290 and SRP029453. Sequenced stocks were deposited in the University of California, San Diego (UCSD) stock center with stock numbers 14021-0261.38- 14021-0261.51 and 14021-0251.293- 14021-0251.311.

Acknowledgements

We would like to thank Elizabeth G. King, Anthony D. Long, and Alexis S. Harrison, and Trevor Bedford for helpful discussions, as well as Portola Coffee Labs for a supportive writing environment. J. J. Emerson gave valuable advice on the use of lastz and the UCSC toolkit. B. Ballard shared *D. simulans* fly stocks collected from Madagascar. We would also like to thank several anonymous reviewers whose comments substantially improved the manuscript. This work is supported by a National Institute of General Medical Sciences at the National Institute of Health Ruth Kirschstein National Research Service Award F32-GM099377 to RLR. Research funds were provided by National Institute of General Medical Sciences at the National Institute of Health grant R01-GM085183 to KRT and R01-GM083228 to PA. All sequencing and PacBio library preparations were performed at the UC Irvine High Throughput Genomics facility, which is supported by the National Cancer Institute of the National Institutes of Health under Award Number P30CA062203. The content is solely the responsibility of the authors and does not necessarily represent the official views of the National Institutes of Health. The funders had no role in study design, data collection and analysis, decision to publish, or preparation of the manuscript.

Bibliography

- Alkan C, Kidd JM, Marques-Bonet T, et al. (13 co-authors). 2009. Personalized copy number and segmental duplication maps using next-generation sequencing. *Nat. Genet.* 41:1061–1067.
- Altschul SF, Gish W, Miller W, Myers EW, Lipman DJ. 1990. Basic Local Alignment Search Tool. *Journal of Molecular Biology.* 215:403–410.
- Andolfatto P. 2001. Contrasting patterns of X-linked and autosomal nucleotide variation in *Drosophila melanogaster* and *Drosophila simulans*. *Mol. Biol. Evol.* 18:279–290.
- Andolfatto P, Wong KM, Bachtrog D. 2011. Effective population size and the efficacy of selection on the X chromosomes of two closely related *Drosophila* species. *Genome Biol Evol.* 3:114–128.
- Bachtrog D, Thornton K, Clark A, Andolfatto P. 2006. Extensive introgression of mitochondrial DNA relative to nuclear genes in the *Drosophila yakuba* species group. *Evolution.* 60:292–302.
- Barrett RD, Schluter D. 2008. Adaptation from standing genetic variation. *Trends Ecol. Evol. (Amst.)*. 23:38–44.
- Bolstad BM, Irizarry RA, Astrand M, Speed TP. 2003. A comparison of normalization methods for high density oligonucleotide array data based on variance and bias. *Bioinformatics.* 19:185–193.
- Cardoso-Moreira M, Arguello JR, Clark AG. 2012. Mutation spectrum of *Drosophila* CNVs revealed by breakpoint sequencing. *Genome Biol.* 13:R119.
- Cardoso-Moreira M, Emerson JJ, Clark AG, Long M. 2011. *Drosophila* duplication hotspots are associated with late-replicating regions of the genome. *PLoS Genet.* 7:e1002340.
- Chaisson MJ, Tesler G. 2012. Mapping single molecule sequencing reads using basic local alignment with successive refinement (BLASR): application and theory. *BMC Bioinformatics.* 13:238.

- Charlesworth B. 2012. The role of background selection in shaping patterns of molecular evolution and variation: evidence from variability on the *Drosophila* X chromosome. *Genetics*. 191:233–246.
- Charlesworth B, Coyne J, Barton N. 1987. The relative rates of evolution of sex chromosomes and autosomes. *American Naturalist*. pp. 113–146.
- Conant GC, Wolfe KH. 2008. Turning a hobby into a job: how duplicated genes find new functions. *Nat. Rev. Genet.* 9:938–950.
- Conrad DF, Pinto D, Redon R, et al. (28 co-authors). 2010. Origins and functional impact of copy number variation in the human genome. *Nature*. 464:704–712.
- Corbett-Detig RB, Cardeno C, Langley CH. 2012. Sequence-based detection and breakpoint assembly of polymorphic inversions. *Genetics*. 192:131–137.
- Cridland JM, Macdonald SJ, Long AD, Thornton KR. 2013. Abundance and distribution of transposable elements in two *Drosophila* QTL mapping resources. *Mol. Biol. Evol.* 30:2311–2327.
- Cridland JM, Thornton KR. 2010. Validation of rearrangement break points identified by paired-end sequencing in natural populations of *Drosophila melanogaster*. *Genome Biol Evol.* 2:83–101.
- Adams et al. 2000. The genome sequence of *Drosophila melanogaster*. *Science*. 287:2185–2195.
- Dopman EB, Hartl DL. 2007. A portrait of copy-number polymorphism in *Drosophila melanogaster*. *Proc. Natl. Acad. Sci. U.S.A.* 104:19920–19925.
- Drosophila Twelve Genomes Consortium. 2007. Evolution of genes and genomes on the *Drosophila* phylogeny. *Nature*. 450:203–218.
- Emerson JJ, Cardoso-Moreira M, Borevitz JO, Long M. 2008. Natural selection shapes genome-wide patterns of copy-number polymorphism in *Drosophila melanogaster*. *Science*. 320:1629–1631.
- Ewing B, Green P. 1998. Base-calling of automated sequencer traces using phred. II. Error probabilities. *Genome Res.* 8:186–194.
- Eyre-Walker A, Keightley PD, Smith NG, Gaffney D. 2002. Quantifying the slightly deleterious mutation model of molecular evolution. *Mol. Biol. Evol.* 19:2142–2149.
- Haddrill PR, Bachtrog D, Andolfatto P. 2008. Positive and negative selection on noncoding DNA in *Drosophila simulans*. *Mol. Biol. Evol.* 25:1825–1834.
- Hahn MW, Han MV, Han SG. 2007. Gene family evolution across 12 *Drosophila* genomes. *PLoS Genetics*. 3:e197.

- Harris RS. 2007. Improved pairwise alignment of genomic DNA. Ph.D. thesis, The Pennsylvania State University.
- Hu TT, Eisen MB, Thornton KR, Andolfatto P. 2012. A second generation assembly of the *Drosophila simulans* genome provides new insights into patterns of lineage-specific divergence. *Genome Res.* .
- Hu X, Worton RG. 1992. Partial gene duplication as a cause of human disease. *Hum. Mutat.* 1:3–12.
- Huddleston J, Ranade S, Malig M, et al. (14 co-authors). 2014. Reconstructing complex regions of genomes using long-read sequencing technology. *Genome Res.* .
- Inaki K, Liu ET. 2012. Structural mutations in cancer: mechanistic and functional insights. *Trends Genet.* 28:550–559.
- Ionita-Laza I, Rogers AJ, Lange C, Raby BA, Lee C. 2009. Genetic association analysis of copy-number variation (CNV) in human disease pathogenesis. *Genomics.* 93:22–26.
- Jones CD, Begun DJ. 2005. Parallel evolution of chimeric fusion genes. *Proceedings of the National Academy of Sciences, USA.* 102:11373–11378.
- Jones CD, Custer AW, Begun DJ. 2005. Origin and evolution of a chimeric fusion gene in *Drosophila subobscura*, *D. madeirensis* and *D. guanche*. *Genetics.* 170:207–219.
- Kearney HM, Kirkpatrick DT, Gerton JL, Petes TD. 2001. Meiotic recombination involving heterozygous large insertions in *Saccharomyces cerevisiae*: formation and repair of large, unpaired DNA loops. *Genetics.* 158:1457–1476.
- Kent WJ, Baertsch R, Hinrichs A, Miller W, Haussler D. 2003. Evolution’s cauldron: duplication, deletion, and rearrangement in the mouse and human genomes. *Proc Natl Acad Sci USA.* 100:11484–9.
- Korbel JO, Urban AE, Affourtit JP, et al. (23 co-authors). 2007. Paired-end mapping reveals extensive structural variation in the human genome. *Science.* 318:420–426.
- Lazarro B, Clark A. 2012. Rapidly Evolving Genes and Genetic Systems, chapter Rapid evolution of innate immune response genes. In: R.S. Singh and Kulathinal (2012).
- Lee YC, Reinhardt JA. 2012. Widespread polymorphism in the positions of stop codons in *Drosophila melanogaster*. *Genome Biol Evol.* 4:533–549.
- Li H, Durbin R. 2009. Fast and accurate short read alignment with Burrows-Wheeler transform. *Bioinformatics.* 25:1754–1760.
- Li H, Handsaker B, Wysoker A, Fennell T, Ruan J, Homer N, Marth G, Abecasis G, Durbin R. 2009. The Sequence Alignment/Map format and SAMtools. *Bioinformatics.* 25:2078–2079.

- Liang Q, Conte N, Skarnes WC, Bradley A. 2008. Extensive genomic copy number variation in embryonic stem cells. *Proc. Natl. Acad. Sci. U.S.A.* 105:17453–17456.
- Lim JK, Simmons MJ. 1994. Gross chromosome rearrangements mediated by transposable elements in *Drosophila melanogaster*. *Bioessays*. 16:269–275.
- Long M, Langley CH. 1993. Natural selection and the origin of *jingwei*, a chimeric processed functional gene in *Drosophila*. *Science*. 260:91–95.
- Mackay TF, Richards S, Stone EA, et al. (52 co-authors). 2012. The *Drosophila melanogaster* Genetic Reference Panel. *Nature*. 482:173–178.
- Mills RE, Walter K, Stewart C, Handsaker RE, Chen ea K. 2011. Mapping copy number variation by population-scale genome sequencing. *Nature*. 470:59–65.
- Ohshima K, Igarashi K. 2010. Inference for the initial stage of domain shuffling: tracing the evolutionary fate of the *PIPSL* retrogene in hominoids. *Molecular Biology and Evolution*. 27:2522–2533.
- Petrov DA, Lozovskaya ER, Hartl DL. 1996. High intrinsic rate of DNA loss in *Drosophila*. *Nature*. 384:346–349.
- Presgraves DC. 2008. Sex chromosomes and speciation in *Drosophila*. *Trends Genet.* 24:336–343.
- Ranz JM, Castillo-Davis CI, Meiklejohn CD, Hartl DL. 2003. Sex-dependent gene expression and evolution of the *Drosophila* transcriptome. *Science*. 300:1742–1745.
- Rogers RL, Bedford T, Hartl DL. 2009. Formation and longevity of chimeric and duplicate genes in *Drosophila melanogaster*. *Genetics*. 181:313–322.
- Rogers RL, Hartl DL. 2012. Chimeric genes as a source of rapid evolution in *Drosophila melanogaster*. *Mol. Biol. Evol.* 29:517–529.
- RS Singh JX, Kulathinal R, editors. 2012. *Rapidly Evolving Genes and Genetic Systems*. Oxford: Oxford University Press.
- Sawyer SA, Hartl DL. 1992. Population genetics of polymorphism and divergence. *Genetics*. 132:1161–1176.
- Schrider DR, Houle D, Lynch M, Hahn MW. 2013. Rates and genomic consequences of spontaneous mutational events in *Drosophila melanogaster*. *Genetics*. 194:937–954.
- Sudmant PH, Kitzman JO, Antonacci F, Alkan C, Malig ea M. 2010. Diversity of human copy number variation and multicopy genes. *Science*. 330:641–646.
- Tuzun E, Sharp AJ, Bailey JA, et al. (12 co-authors). 2005. Fine-scale structural variation of the human genome. *Nat. Genet.* 37:727–732.

- Viterbi A. 1967. Error bounds for convolutional codes and an asymptotically optimum decoding algorithm. *IEEE Transactions on Information Theory*. IT-13:260–269.
- Wong A, Wolfner M. 2012. Rapidly Evolving Genes and Genetic Systems, chapter Evolution of *Drosophila* seminal proteins and their networks. In: R.S. Singh and Kulathinal (2012).
- Wright S. 1931. Evolution in Mendelian Populations. *Genetics*. 16:97–159.
- Xie C, Tammi MT. 2009. CNV-seq, a new method to detect copy number variation using high-throughput sequencing. *BMC Bioinformatics*. 10:80.
- Ye K, Schulz MH, Long Q, Apweiler R, Ning Z. 2009. Pindel: a pattern growth approach to detect break points of large deletions and medium sized insertions from paired-end short reads. *Bioinformatics*. 25:2865–2871.
- Zhang J, Dean AM, Brunet F, Long M. 2004. Evolving protein functional diversity in new genes of *Drosophila*. *Proceedings of the National Academy of Sciences, USA*. 101:16246–16250.
- Zhang Y, Lu S, Zhao S, Zheng X, Long M, Wei L. 2009. Positive selection for the male functionality of a co-retroposed gene in the hominoids. *BMC evolutionary biology*. 9:252.
- Zhou Q, Zhang G, Zhang Y, Xu S, Zhao R, Zhan Z, Li X, Ding Y, Yang S, Wang W. 2008. On the origin of new genes in *Drosophila*. *Genome Research*. 18:1446–1455.
- Zichner T, Garfield DA, Rausch T, Stutz AM, Cannavo E, Braun M, Furlong EE, Korb JO. 2013. Impact of genomic structural variation in *Drosophila melanogaster* based on population-scale sequencing. *Genome Res*. 23:568–579.

Table 1: Duplicated Regions in *D. yakuba* and *D. simulans*

	<i>D. yakuba</i>	<i>D. simulans</i>
Whole gene	248	296
Partial gene	745	462
Intergenic	745	577

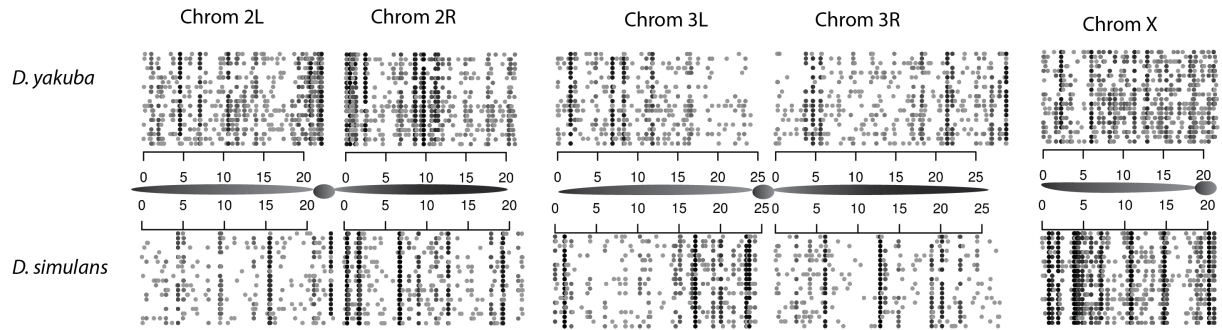


Figure 1: Tandem duplications in 20 sample strains of *D. yakuba*. Regions spanned by divergently-oriented reads are shown with sample strains plotted on different rows, whereas axes list genomic location in Mbp. Duplications are more common around the centromeres, especially on chromosome 2. Frequencies are shaded in greyscale according to frequency, with high frequency variants shown in solid black. The *D. simulans* X chromosome appears to have an excess of high frequency variants in comparison to the *D. simulans* autosomes and the *D. yakuba* X chromosome.

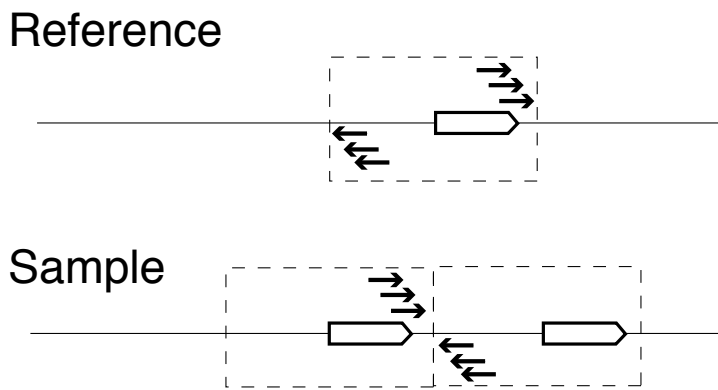


Figure 2: A tandem duplication in a sample that was then used to generate paired-end Illumina libraries. Duplications should be apparent through divergently-oriented read pairs when mapping onto the reference genome. Tandem duplications require a minimum of three divergently-oriented read pairs. Duplication span is recorded as the minimum and maximum coordinates spanned by divergent reads.

Duplication on 3L

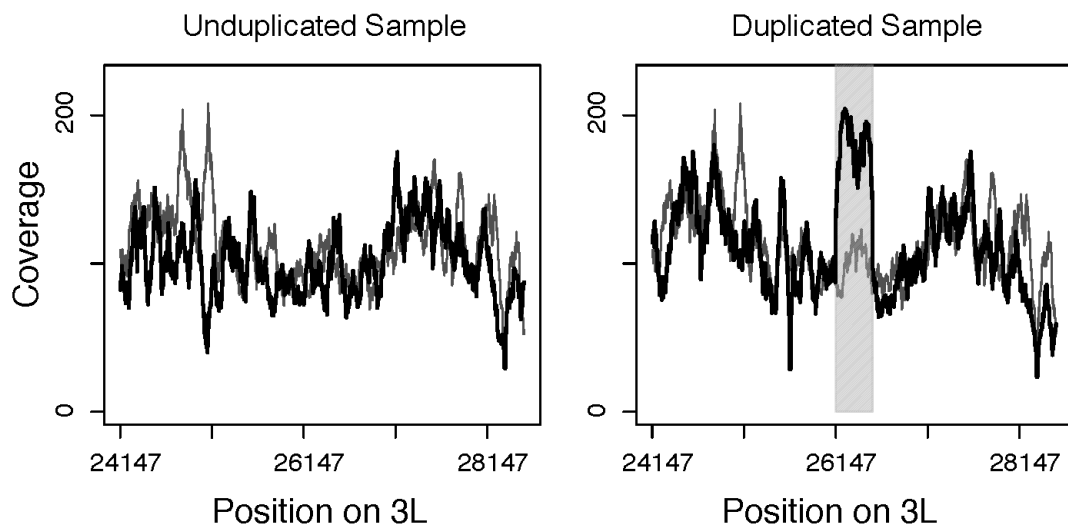


Figure 3: Coverage change for a duplication on chromosome 3L in Line 9 of *D. yakuba*. Regions spanned by divergently-oriented reads are shaded. Sample coverage is shown in black, while reference genome coverage is shown in grey.

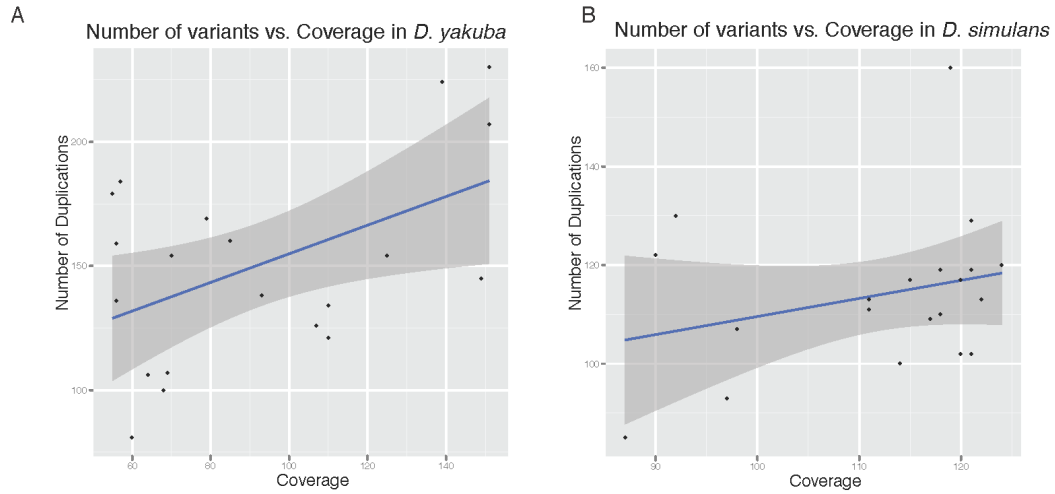


Figure 4: Number of variants vs. coverage by line in *D. yakuba* (A) and *D. simulans* (B). Regression line (blue) and 95% CI (grey) are shown. Correlation between coverage and number of duplications is low (*D. yakuba* adjusted $R^2 = 0.21$, *D. simulans* adjusted $R^2 = 0.03$).

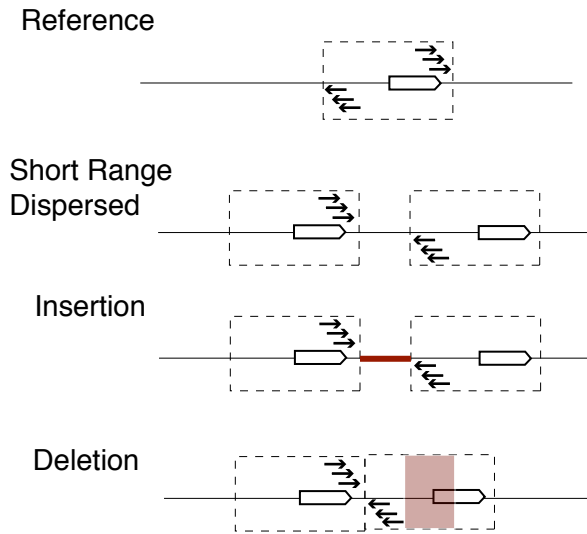


Figure 5: Complex breakpoints and subsequent modification of tandem duplications. Short range dispersed duplications, duplication with insertion of novel sequence, and duplication with subsequent deletion will all display the same signals of divergently-oriented reads. While all of these indicate duplication has occurred, signals solely from short sequence read pairs are unlikely to capture the full complexity of duplication events.

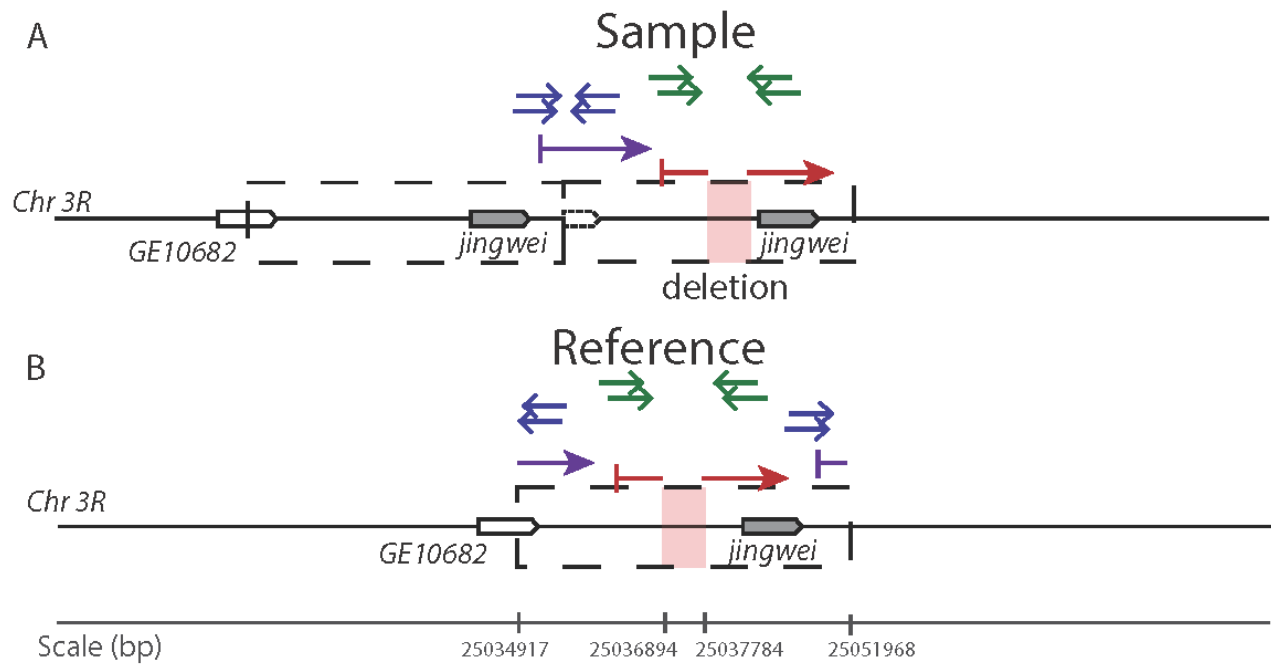


Figure 6: Read mapping patterns indicative of a modified duplication surrounding *jingwei* in *D. yakuba* line NY66-2. Duplications are indicated with divergently-oriented paired-end reads (blue) as well as with split read mapping of long molecule sequencing (purple). Deletions in one copy are suggested by gapped read mapping of long molecule reads (red) as well as multiple long-spanning read pairs at the tail of mapping distances in paired-end read sequencing (green) just upstream from *jgw*. Up to 20% of duplicates observed have long-spanning read pairs indicative of putative deletions in one or more alleles in the population.

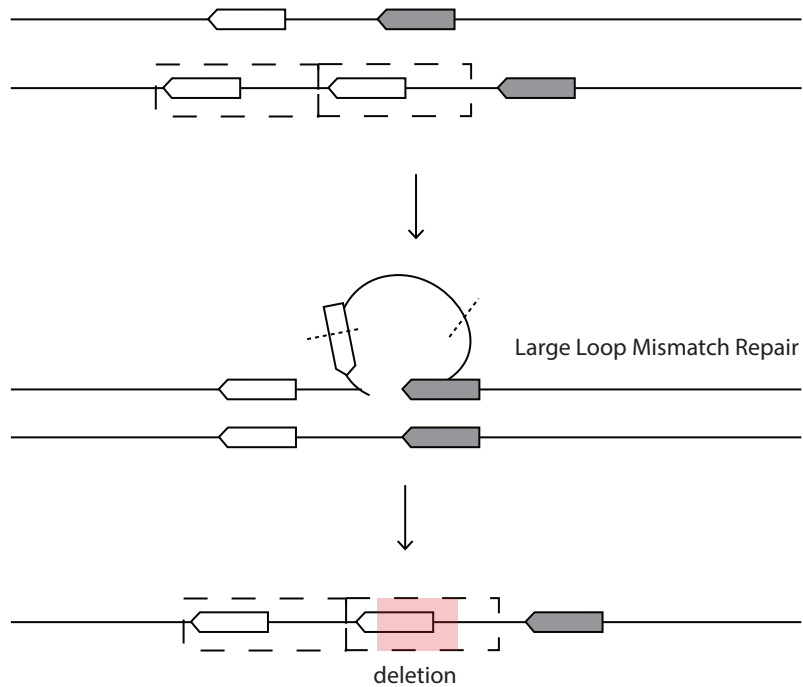


Figure 7: Secondary Deletion via large loop mismatch repair. A tandem duplication forms via ectopic recombination or replication slippage. At some point prior to fixation in the population the duplication pairs with an unduplicated chromatid in meiosis or mitosis, invoking the action of the large loop mismatch repair system. Imprecise excision results in a modified duplicate with partially deleted sequence. Large loop mismatch repair requires that duplications are polymorphic, and would therefore produce secondary modification over short timescales, resulting in rapid modification of tandem duplicates.

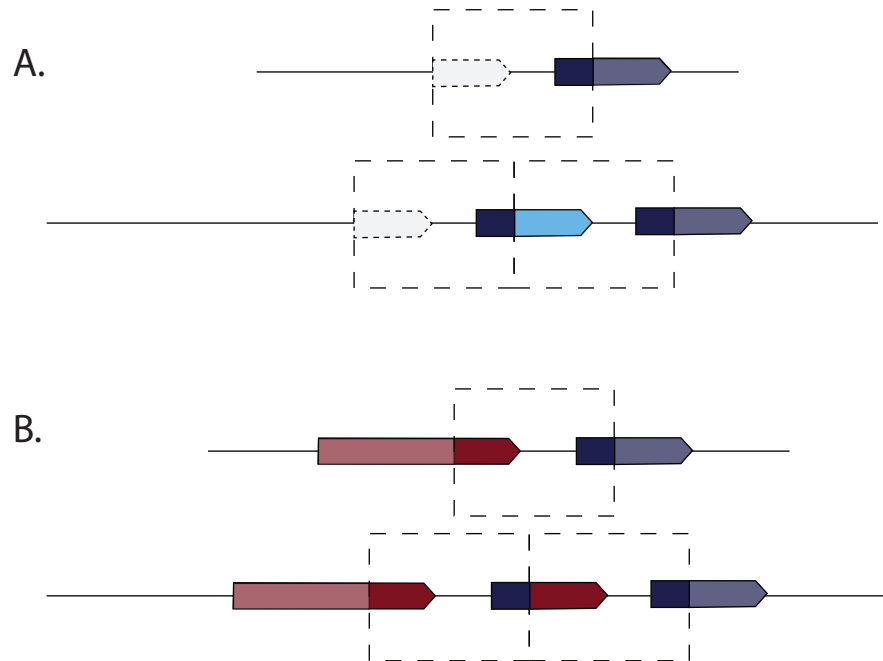


Figure 8: Abnormal Gene Structures. Duplicated sequence is highlighted with bold colors and is framed by the dashed box. A) The partial duplication of a coding sequence (blue) results in the recruitment of previously upstream non coding sequence (dashed lines) to create a novel open reading frame (blue and turquoise). B) Tandem duplication where both boundaries fall within coding sequences results in a chimeric gene.

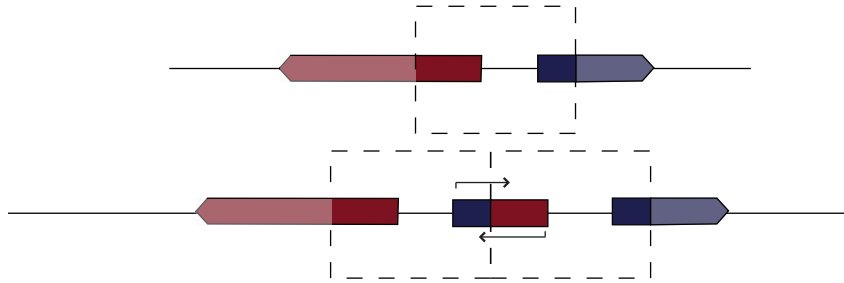


Figure 9: Dual promoter genes. Duplicated sequence is highlighted with bold colors and is framed by the dashed box. Tandem duplication where both boundaries fall within coding sequences results in a chimeric gene which contains two promoters, one which facilitates transcription in one direction, the other facilitating transcription from the opposite strand. The chimera is capable of making partial anti-sense transcripts.

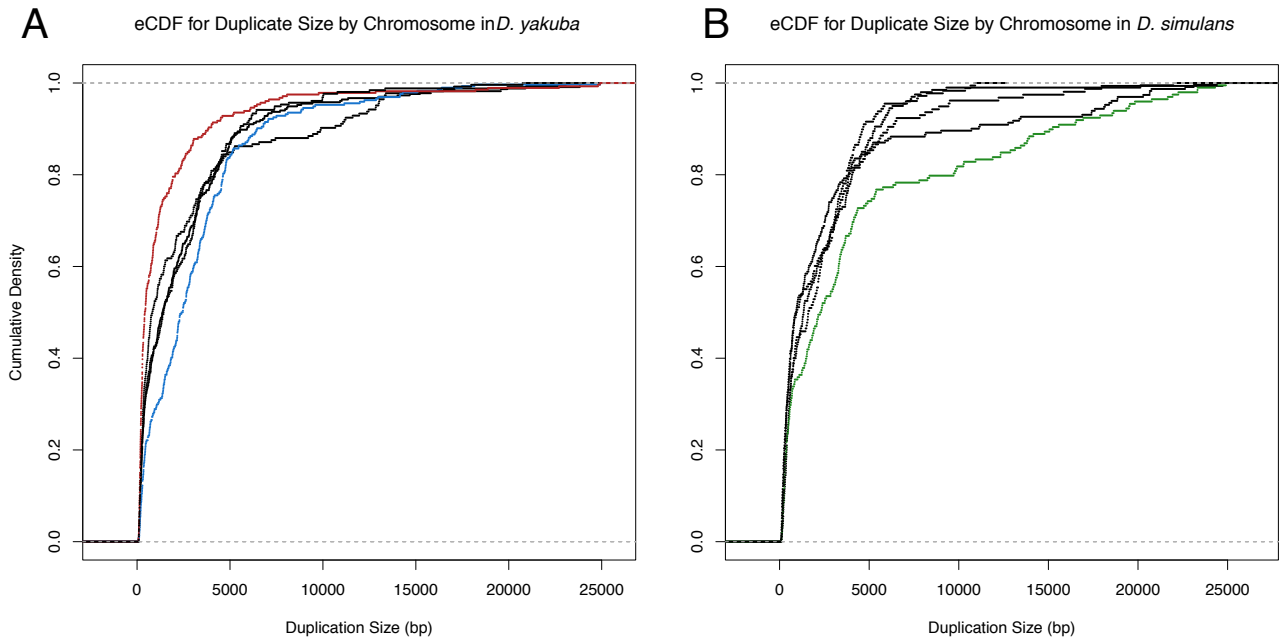


Figure 10: Cumulative distribution function for duplication sizes for the X and 4 major autosomal arms in A) *D. yakuba* and B) *D. simulans*. The X chromosome in *D. yakuba* (red) is significantly different from all autosomes ($P < 10^{-3}$) due to a large number of small duplications 500 bp or less. Chromosome 2R (blue) is also different from Chr2L and 3R ($P < 0.05$). In *D. simulans* chromosome 3L (green) is significantly different 2L, 3R, and the X.

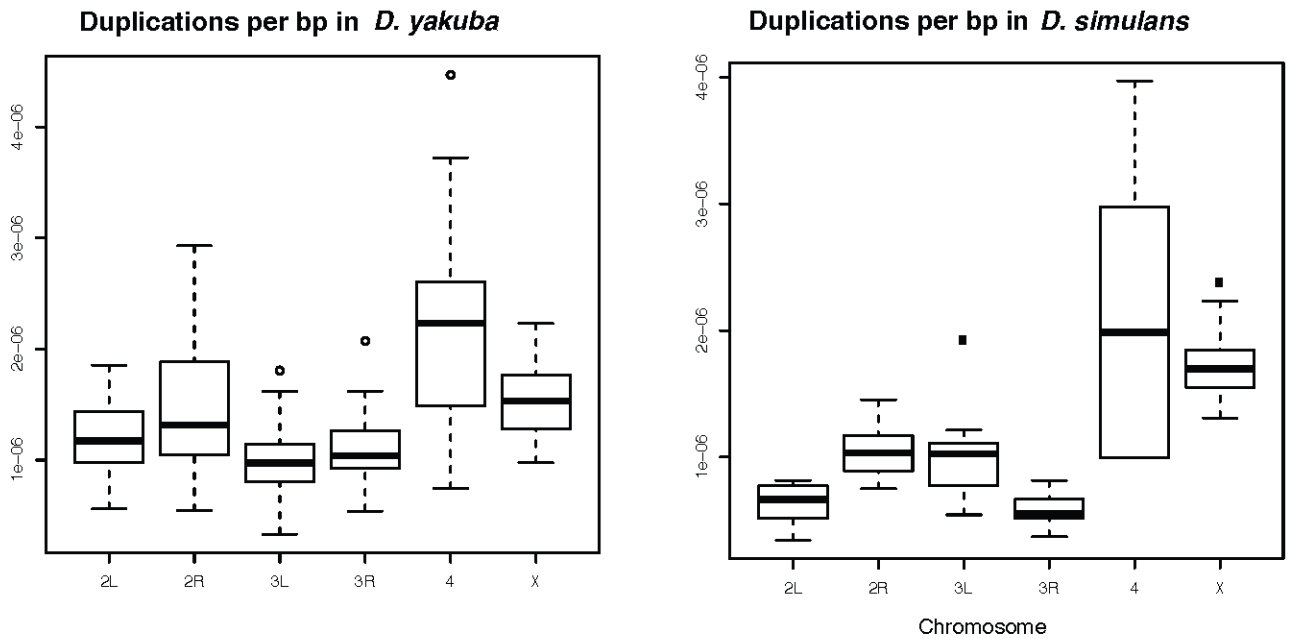


Figure 11: Number of Duplications per bp on the X and major autosomes in *D. yakuba* and *D. simulans*. The X chromosome in *D. simulans* contains an excess of duplications in comparison with the autosomes. Chromosome 2R also contains more duplications per bp than chromosome 3R but no other autosomes are significantly different. Chromosome 4, the dot chromosome, has more duplications per mapped bp in both *D. yakuba* and *D. simulans* than any other chromosome.

Supporting Information

Illumina sequencing and mapping

The genomic DNA (gDNAs) used for the library preparations were extracted with the Genra Puregene Cell Kit including the RNase A Solution (Qiagen) or the reagents from the Puregene Accessories (Qiagen, as indicated below). The extraction and purification procedures were modified from the protocol for *D. melanogaster* (Qiagen Supplementary Protocol) and combined with column purification (Zymo) as described below, to give better and more constant yields with higher throughput.

About 15 frozen (-80°C) female flies of each fly line were homogenized into small pieces in cold 300 μ L Cell Lysis Solution (158906, Qiagen), and then incubated for 15min at room temperature. The RNAs were digested by 4.5 μ L RNase A Solution (158922, Qiagen) and incubated for 15min at 37°C. The contaminated proteins were precipitated by mixing with 100 μ L Protein Precipitation Solution (158910, Qiagen) and centrifuged 4min at 16,000g. The extracted gDNAs in the supernatant were column purified with the DNA Clean and Concentrator 25 Kit (D4013, Zymo) followed its protocol, using 5 volumes of Binding Buffer. The quality of these purified gDNAs were checked with 1% agarose gel, showed intact size of about 10 kb without degraded lower bands.

About 3 μ g purified gDNAs in 100 μ L EB (Elution Buffer, 10mM Tris, pH8.5, Invitrogen) were sheared with Covaris at 300 bp setting and purified with Purelink PCR Purification (HC) Kit (K3100-01, Invitrogen), followed their protocols respectively. The distributions of these fragments of about 300-1000 bp were confirmed with 2% agarose gel.

The purified fragments were end-repaired for 30min at 25°C with Quick Blunting Kit (E0542L, NEB), A-tailed for 30min at 37°C with Klenow Fragments (M02112L, NEB) and dATP (R0141, Fermentas), ligated to adaptors (see below) for 10min at 25°C with Quick Ligation Kit (E0542L, NEB), size selected between 350 bp to 450 bp on 2% agarose gel Seakem LE (5000, Lonza) and extracted with ZymoClean Gel DNA Recover Kit (D4001, Zymo), and PCR amplified 15 cycles by Phusion High-Fidelity DNA Polymerase (M0530S, NEB) with dNTP (N0447L, NEB) and Primers (see below), followed these reagents protocols respectively. The DNA Clean and Concentrator-5 Kits (D4013, Zymo) were used to purify the product after each reaction.

The libraries showed a band between 400 bp to 500 bp on 2% agarose gel. All concentrations through the preparation were measured with Qubit Fluorometer (Invitrogen). Final libraries were diluted to 10nM before sequencing, based on the reads from Qubit and

the sizes from agarose gel.

Adapters and PCR Primers for Paired-End Library: All adapters and primers were HPLC purified and ordered from Integrated DNA Technologies (IDT):

PE-Ad1, 5'-/5Phos/GATCGGAAGAGCGGTTCAGCAGGAATGCCGAG

PE-Ad2, 5'-ACACTCTTTCCCTACACGACGCTCTTCCGATC*T

PE-PCR, (1) 5'-AATGATACGGCGACCACCGAGATCTACACTCTTTCCCTACACGACGCTCTTCCGATC*T

PE-PCR, (2) 5'-CAAGCAGAAGACGGCATACGAGATCGGTCTCGGCATTCTGCTGAACCGCTCTTCCGATC*T

HMM Parameters

Emission probabilities were defined using the probability density function of each respective normal distribution as below:

$$E_{deletion} = p(\text{SampleCoverage} - \text{ReferenceCoverage}) \sim N(-\mu_{Ref}, 2\sigma_{Ref}^2)$$

$$E_{singleton} = p(\text{SampleCoverage} - \text{ReferenceCoverage}) \sim N(0, 2\sigma_{Ref}^2)$$

$$E_{duplicate} = p(\text{SampleCoverage} - \text{ReferenceCoverage}) \sim N(\mu_{Ref}, 2\sigma_{Ref}^2)$$

$$E_{triplicate} = p(\text{SampleCoverage} - \text{ReferenceCoverage}) \sim N(2\mu_{Ref}, 2\sigma_{Ref}^2)$$

Where μ_{Ref} and σ_{Ref} are the mean and standard deviation, respectively, for quantile normalized coverage in the reference strain for the window being evaluated. In each iteration, the most likely path was predicted using the Viterbi algorithm (Viterbi 1967), which identifies the most probable path for an HMM.

Initial state probabilities were set according to π_0 and initial transition probabilities were set according to T_0 , where row and column indices ranging from 0 to 3 are indicative of copy number. Initial probabilities are set such that the singleton state is initially most likely and states are initially most likely to remain constant during transitions.

$$\pi_0 = [0.07 \quad 0.79 \quad 0.07 \quad 0.07]$$

$$T_0 = \begin{bmatrix} 0.79 & 0.07 & 0.07 & 0.07 \\ 0.07 & 0.79 & 0.07 & 0.07 \\ 0.07 & 0.07 & 0.79 & 0.07 \\ 0.07 & 0.07 & 0.07 & 0.79 \end{bmatrix}$$

HMM parameters of transition probabilities (T) and state likelihoods (π) were optimized using Expectation Maximization based on the Viterbi predictions for each individual window until a steady state was reached. Emission probability distributions were not updated as data in a given window will often be insufficient for one or more underlying states. Coverage can change substantially from one region of the genome to another, and so state calls were estimated for 4 kb windows. For larger windows, the variance in reference coverage across the window can render the emission probabilities less sensitive, and smaller windows can result in insufficient data to obtain adequate likelihoods.

Transition probabilities serve to ground HMM output such that low transition probabilities lower the likelihood of state changes, resulting in smoother calls. However in extreme cases low estimated transition probabilities can have an extreme chilling effect such that they will overwhelm the emission probabilities. The minimum transition probability for any given state change was therefore set at $p = 0.07$. Minimum transition probabilities below a threshold of 0.05 can have a massive effect on the number of duplicated sites, but varying minimum transition probabilities between 0.05 and 0.15 have only a minor effect. Similarly the minimum state probability was set to 0.00025 for all states and minimum emission probability was set to 10^{-10} to avoid zero probabilities.

Coverage can be highly stochastic and will depend on the amount of divergence between sample and reference, GC content, sequence complexity, and uniformity of error rates across sites. Requiring a more stringent mapping quality results in substantial coverage changes for many sites (Table S4). For even moderately divergent paralogs, higher mapping quality thresholds can greatly diminish our ability to observe two-fold increases in coverage.

In some cases, highly divergent paralogs may not display increases in coverage at all, and in other cases high variance in reference strain coverage may make automated detection of elevated coverage in samples extremely difficult. Many duplicated variants also show clear elevated coverage for a large portion of the region spanned by divergently-oriented reads, with drops in other regions. Whether these represent cases where reads fail to map due to divergence or whether they are subsequent deletion at duplicated sites through replication slippage or through the large-loop mismatch repair system remains ambiguous. Examples of these problematic regions are included in Figure S4. Additionally, duplicated regions that are substantially smaller than the 325 bp Illumina library insert size may not be identified easily using divergent read calls, but should be readily apparent in coverage changes. Hence, there may be some disparity between the HMM output and divergent read calls, especially for very small or highly divergent duplications.

Some previous CNV calling schemes have not taken advantage of HMM models, but rather have simply relied on regions of high coverage relative to the genome average (Alkan et al. 2009). These schemes cannot correct for local variation in coverage due to base composition or potential for mismapping, nor do they correct for natural variation in coverage across genomic regions. Moreover, such models risk a high false positive rate among genomes with low levels of genomic duplication and high false negative rates for genomes that display rampant duplication. We observe substantial variation in coverage across sites within the reference, which is naturally accounted for in the HMM emission probabilities without the need for additional models or coverage corrections.

Previous work, especially analysis of microarrays, has clustered probes with two-fold coverage increases as indicative of a single duplication provided that they fell within a specific threshold distance (Emerson et al. 2008, Dopman and Hartl 2007, Conrad et al. 2010). Given the sparseness of microarray probes, such methods are prone to misidentify multiple duplications in a larger window as single duplications that span large sections of the genome. However, given the precision provided by Illumina resequencing, we are able to identify increased coverage at individual sites, which in combination with divergently-oriented reads

should allow us to identify duplications with greater precision and increased ability to identify multiple small duplications that lie adjacent to one another.

Sample coverage

Illumina reads from the *D. simulans* reference stock consist of a single lane of paired-end data with a 104 bp read length, resulting in a median coverage of 55X (considering only the major chromosome arms X, 2L, 2R, 3L, 3R, and 4) when aligned to the assembly described in (Hu et al. 2012). The remaining 41 samples were sequenced with two to three lanes of paired-end sequencing, with read lengths being a mix of primarily 54 bp and 76 bp (Tables S2 and S1). Illumina reads cover 116 Mbp of the *D. simulans* reference and 99 Mbp of the *D. yakuba* reference (Table S3) The total sequencing thus consists of 123 lanes of Illumina data. Table S4 shows summary statistics of the sequencing at various mapping quality (Li and Durbin 2009) cutoffs. With no quality filters, median coverage of the major arms ranges from 55x to 151x, covering > 98% of the genome with 95% of sites with non-zero coverage having a coverage ≥ 7 (Table S4). The variation in coverage from sample to sample, and the overall higher coverage in *D. simulans* compared to *D. yakuba* reflects the order in which the samples were sequenced. As the sequencing effort progressed, the throughput for Illumina runs increased, while the number of lanes and read length per lane were held constant, resulting in higher coverage.

Median raw coverage for the *D. yakuba* reference genome was 115X with a standard deviation of 404.25 and a range from 0 to 281347, whereas median raw coverage in the *D. simulans* reference was 55x with a standard deviation of 109.44 and a range from 0 to 8073 (Figure S6). While some regions have abnormally high coverage that inflates the standard deviation, the majority of the genome is sequenced to between 0 and 400X in both species (Figure S6). Excluding sites with raw coverage greater than 400X yields a median of 114X and a standard deviation of 54.99 in the *D. yakuba* references and a median of 55 and a standard deviation of 28.80 in the *D. simulans* reference. Distributions of raw coverage were highly similar for all strains (Figure S2, S3).

Increasing quality filters results in modest changes in median coverage, but has a noticeable effect on the number of sites with a coverage of zero ($f_{0,X}$) and on the first quantile of coverage for sites with coverage greater than zero ($Q_{1,X}$, Table S4). These data would suggest that a large number of sites with single digit raw coverage in the reference may be the product of sequencing errors and mismapping. The affect of imposing additional map quality filters is stronger in sample strains than in the reference (Table S4) and can impede mappings in the face of even a small number of mismatches. Hence, for all analyses of coverage changes in sample strains relative to reference, we used coverage with no additional quality filters, a factor that is essential in detecting increased coverage for even modestly diverged regions. Targeted insert size for Illumina libraries was 325 bp, median fragment size by line ranges from 270 bp-532 bp (Table S5).

***In silico* confirmation of rearrangements**

***De novo* assembly of breakpoints**

A putative tandem duplication results in the formation of a single novel sequence junction (Cridland and Thornton 2010; Figure S7). Reads mapping to this novel junction will fail to map to an existing reference genome Mackay et al. (2012). We mined the both the divergently-oriented reads and mapped/unmapped read pairs from the putative breakpoint region (Figure S8A) using `samtools` version 0.1.18 Li et al. (2009) and fed them into `phrap` version 1.090518 (<http://www.phrap.org>) for assembly. We used the following parameters for `phrap`: `-vector_bound 0 -forcelevel 10 -minscore 10 -minmatch 10 -new_ace -bypasslevel 1 -maxgap 45 -revise_greedy -force_high`.

Homology searches using `lastz`

The contigs obtained from `phrap` were then subjected to a homology search against the reference genome using `lastz` version 1.02.00 (<http://www.bx.psu.edu/~rsharris/lastz/>) Harris (2007), and the resulting alignments chained together using `axtChain` and parsed with `chainNet` Kent et al. (2003). These latter two tools combine the alignments from `lastz` to find the highest-scoring colinear alignment of a query to a target, and then separate alignments into separate files by target, respectively. A single contig chaining within Xbp of the regions identified by divergently-oriented reads as flanking the breakpoints was considered to have confirmed the existence of the event. In practice, we let X equal 0, 50, or 100 base pairs.

CNV calling

We identify 38 divergent read calls consistent with tandem duplications in the *D. yakuba* reference strain, 20 of which are specific to the reference strain. Meanwhile the *D. simulans* reference strain has 92 divergent calls in the reference strain, 29 of which are specific to the reference. These unannotated duplicates in the reference sequence were excluded from downstream analyses on the grounds that they are likely to be biased with respect to gene content, genomic location, base composition, and population frequency. Excluding unannotated duplicates in the reference and putative ancestral duplications, *D. yakuba* has an average of 148.6 duplications per strain with a standard deviation of 41.7, while in *D. simulans* we find 113 duplications per strain with a standard deviation of only 15.6 (Table S6) and a weak correlation between coverage and number of variants per strain (Figure 4). Hence the variance in number of duplications per strain is 7.5x greater in *D. yakuba*, in addition to strains harboring on average greater numbers of tandem duplications. Corresponding numbers with reference duplicates and ancestral duplications included are found in Table S7. The distribution of read pair depth indicating events for a representative sample strain, CY20A, is in Figure S1.

We used a Hidden Markov Model that compares coverage in genomic resequencing of the reference to observed coverage in reference strains to identify regions with elevated coverage consistent with duplication of sequences spanned by divergently-oriented reads. Coverage was quantile normalized prior to analysis so that each strain displays equal mean and variance, rendering tests of differential coverage robust in the face of differing sequence depth across samples or across sites (Bolstad et al. 2003).

In some cases, a duplication may in fact exist, but due to lower sequencing coverage in one strain, or due to stochastic effects of sampling, a duplication may not be identified via paired-end reads. Such false negatives may be more common for variants that are significantly smaller than the library insert size where the likelihood of finding divergently-oriented reads is far lower. To correct the frequency distribution for such false negatives, we used increased coverage to identify duplications in additional strains. For duplications defined using 3 or more pairs of divergently-oriented reads that also showed at least one divergently-oriented read pair as well as two-fold or greater coverage increases in additional strains, frequencies were corrected to include a duplication in that strain.

For *D. yakuba*, frequency correction based on increased coverage resulted in additional calls for 10 duplications across a total of 17 calls in individual strains for duplications larger than 325 bp, yielding a final total of 1033 duplications across 2323 calls in individual strains greater than the targeted library insert size. These estimates suggest that among duplications that can be identified using paired-end reads, the false negative rate is 0.732% ($\frac{17}{2323}$) for duplications larger than the library insert size. For duplications smaller than the targeted library insert size we corrected the frequency estimates for 53 duplications resulting in a total of 91 duplication calls in additional strains. Compared to the total of 691 calls in individual strains across 382 duplications, the false negative rate for duplications smaller than the targeted library insert size is 13.2% ($\frac{91}{691}$) for an overall false negative rate of 3.6% ($\frac{108}{3014}$). In *D. simulans*, corrections result in 14 additional duplication calls across 11 duplicated sites for

duplicates smaller than 325 bp and 4 additional calls across 2 sites for duplicates larger than 325 bp. The resulting false negative rates are 4.3% ($\frac{14}{329}$) for small duplications and 0.20% ($\frac{4}{1964}$) for duplications larger than the library insert size for an overall false negative rate of 0.78% ($\frac{18}{2293}$). Duplicate size and coverage with divergently-oriented reads are not correlated in individual samples ($R = -0.048$, $P = 0.55$) suggesting that methods are unbiased with respect to duplicate size.

We have excluded duplications larger than 25 kb as these are substantially less likely to display increased coverage across the span of divergently-oriented reads. While there may be some duplications larger than 25 kb, such divergently-oriented reads may be caused by within-chromosome translocations or TE movement as well as tandem duplications, and thus the genetic constructs which produce these abnormal mappings are uncertain. We, however, observe no duplications greater than 25 kb which have continuously elevated coverage across the span of divergently-oriented reads, consistent with size limits observed in previous surveys in *D. melanogaster* (Dopman and Hartl 2007).

Confirmation with long sequencing reads

We generated PacBio genomic DNA libraries for four sample strains to roughly 8X coverage. A total of 10ug Qiagen column purified genomic DNA was sheared using a Covaris g-tube according to PacBio. Protocol low-input 10 kb preparation and sequencing (MagBead Station). The Covaris protocol for g-tube was followed (Beckman Allegra 25R centrifuge). AMPure magnetic beads were purchased directly from Beckman and manually washed according to the protocol in Pacific Biosciences Template Preparation and Sequencing Guide. DNA template prep kit 2.0 (3 kb-10 kb) was used for library construction. After construction of the 10 kb SMRTbell template, the concentration was measured by Qubit and the library size analysis performed using an Agilent Bioanalyzer. The Pacific Biosciences calculator (version 1.3.3) determined the amount of sequencing primer to anneal and the amount of polymerase to bind (DNAPolymerase binding kit 2.0). The calculator also recommended sample concentrations for binding the polymerase loaded SMRTbell templates to MagBeads.

The PacBio RS remote version 1.3.3 set up the sequencing reaction by identifying sample wells, sequencing protocol, number of SMRT cells and length of movie. The sequencing protocol was MagBead standard seq v1. Reagents from DNA sequencing kit 2.0 were used for the sequencing protocol. 120 minute movies were taken for each SMRTcell. The SMRT cells were version 3. DNA control complex 2.0 (3 kb-10 kb) was the internal control. Five SMRT cells were analyzed for the 10 kb preparation of *D. yakuba* reference genome. The movie which records the light pulses during nucleotide incorporation is delivered in real time to the primary analysis pipeline which is housed completely in the Blade Center. Proprietary algorithms translate each pulse into bases with a set of quality metrics. The data is then available for secondary analysis. SMRT Portal version v1.4.0 build 118282 with RS_only filter protocol generated the FASTQ files for the sequences and the circular consensus reads (CCS). The default filters were removal of reads <50 bases and less than 0.75 accuracy.

The single-molecule sequencing resulted in an average genomic coverage of 8X for samples CY17C, CY21B3 and NY66, NY73. The entire genome is spanned by only on the order

of 10^7 reads (Table S11), offering low clone-coverage and providing sparse opportunities for confirmation. The detailed results from long-read alignments are shown in Tables S8. The single unconfirmed event in line NY66 has nonzero coverage throughout the duplicated region, but coverage drops to zero immediately 3' of the 3' locus containing divergent short reads and there is evidence of large deletions with respect to the reference, but no single read suggesting a tandem duplication. Thus, only three events were not confirmed (one event per sample), suggesting that our protocol for identifying structural variants using short read data has a 96.1% confirmation rate, and a low false positive rate. For two of these unconfirmed rearrangements we do not have sufficient data to confirm or refute the existence of a rearrangement. Thus, the true false positive rate is likely to be less than the 3.9% implied by these numbers. Thus, single-molecule sequencing suggests that our protocol for detecting tandem duplications via short reads is highly accurate.

Short split read mapping

For comparison of performance (see Results), we ran Pindel version 0.2.5a1 (Ye et al. 2009) with command line options `--max_range_index 4 --RP --report_inversions --report_duplications --report_long_insertions --report_breakpoints --report_close_mapped_reads --min_inversion_size 500 --min_num_matched_bases 20 --additional_mismatch 1 --min_perfect_match_around_BP 3 --sequencing_error_rate 0.05 --maximum_allowed_mismatch_rate 0.02 --anchor_quality 20 --balance_cutoff 100 --window_size 0.01 --minimum_support_for_event 3 --sensitivity 0.99` to identify duplications on each major chromosome arm independently. We required that duplication breakpoints be spanned by at least one read on each strand with a total coverage depth of at least three reads, keeping only calls which map to regions with coverage across all strains. These requirements are somewhat more lenient than the paired read mapping above in that they do not remove putative PCR duplicates, due to a smaller span in which split reads may reasonably be expected to map. Overlap between Pindel and paired-end reads is low, with 11.7% of duplicates (179 of 1415) in *D. yakuba*, as defined by paired-end reads matching duplicates whose breakpoints lie within 100 bp of breakpoints defined by split read mapping of Illumina sequence data (Table S29). These 179 variants capture 102 genes or gene fragments, including 21 whole or nearly whole duplicates ($\leq 90\%$ of CDS span). Only 5 out of 179 (2.7%) are flanked by 30 bp or longer direct repeats in the reference, and none are flanked by 100 bp or longer direct repeats. The site frequency spectra for these confirmed duplicates is also significantly different from that of all duplicates defined by paired-end read mapping ($W = 136270$, $P = 0.0369$).

Yet, we observe a high confirmation rate for duplicates defined by paired-end read orientation, meaning that the false negative rate for Pindel is extremely high. Thus, it would seem that paired-end reads mapping grossly outperforms Pindel for duplications greater than 50 bp when coverage is high. After clustering across strains, requiring that breakpoints in different strains fall within 100 bp of one another, consistent with criteria used for paired-end read orientation, we find 1620 duplications that are not represented among paired-end reads

(Table S29), with an average length of 155 bp, in stark contrast to duplicates defined using paired-end reads, with a maximum span identified solely by Pindel of 5766 bp. Thus, Pindel is likely to outperform paired-end read mapping for extremely small duplications but will perform poorly for duplications larger than the library insert size.

Only 11.7% of duplicates identified with paired end reads are identified through split read mapping (Table S29) (Ye et al. 2009), which is expected with short Illumina reads (Table S1-S2), especially in cases where variants are flanked by repetitive sequence (Text S1). Yet, variants identified through paired end read mapping have a 96.1% confirmation rate with long molecule sequencing. Thus, split read mapping with short sequences has a high false negative rate, and was therefore not used for identification of tandem duplicates or following analyses. In a further attempt to establish precise breakpoints from Illumina sequencing data, we attempted to assemble and confirm *in silico* with short Illumina reads (Text S1, Figure S7-S8). We have reconstructed 49.9% of breakpoints in *D. yakuba* and 58.1% of breakpoints in *D. simulans* that are larger than the 325 bp targeted insert size. Assembly rates increase for larger duplications (Table S30) with 60.3% of breakpoints in *D. yakuba* and 71.5% of breakpoints in *D. simulans* over 1 kb that can be assembled. There are no apparent differences in breakpoint assembly between the X and the autosomes (Table S30) and no significant difference in the frequency spectrum of variants with assembled breakpoints (Figure S9-S10). However, requiring breakpoint reconstruction would eliminate a large amount of the observed variation and likely be biased against repetitive sequences as well as against small variants.

Genome wide surveys

Some regions of the genome cannot be surveyed due to technical limitations. We are unable to identify duplicates flanked by repeats in the reference genome which have zero divergence and are beyond the size limits of our Illumina sequencing library insert size. We identify 121 direct repeats in the *D. yakuba* reference with 99.5% identity to one another which are 300 bp or larger and lie within 25 kb of one another, spanning a total of 678,707 bp (0.57%) of the *D. yakuba* reference (Table S12). In *D. simulans* we identify only 5 such direct repeats, covering 84,055 bp of sequence (0.09%) of the reference sequence (Table S12). In principle, such divergence levels amount to one divergent site per 200 bp, and therefore are expected to be captured with paired end read data. However, these criteria are extremely lenient and offer an upper bound of sequence where repeats might confound duplicate identification. Additionally, duplications whose breakpoints lie within the span of repeats could potentially still be identified, and therefore we did not apply any filters to exclude these regions. These estimates therefore represent an upper bound of sequence in the reference that cannot be readily surveyed. Assuming that the *D. yakuba* reference genome is representative of strains in the population, the number of variants that are unidentified due to repetitive content is likely to be very low.

The methods described here are similarly precluded from surveying sites which have zero coverage across strains and not associated with deletions but are simply a product of stochastic effects of library prep. This filter removes 0.9-1.6% of sequence per strain in

D. simulans and 1.2-1.8% of sequence in *D. yakuba* and will therefore have limited effect. We therefore suggest that the number of tandem duplicates identified via paired end read mapping in high coverage sequencing are therefore likely to be an accurate representation of genome wide variation in the population.

Bibliography

- Alkan C, Kidd JM, Marques-Bonet T, et al. (13 co-authors). 2009. Personalized copy number and segmental duplication maps using next-generation sequencing. *Nat. Genet.* 41:1061–1067.
- Altschul SF, Gish W, Miller W, Myers EW, Lipman DJ. 1990. Basic Local Alignment Search Tool. *Journal of Molecular Biology.* 215:403–410.
- Andolfatto P. 2001. Contrasting patterns of X-linked and autosomal nucleotide variation in *Drosophila melanogaster* and *Drosophila simulans*. *Mol. Biol. Evol.* 18:279–290.
- Andolfatto P, Wong KM, Bachtrog D. 2011. Effective population size and the efficacy of selection on the X chromosomes of two closely related *Drosophila* species. *Genome Biol Evol.* 3:114–128.
- Bachtrog D, Thornton K, Clark A, Andolfatto P. 2006. Extensive introgression of mitochondrial DNA relative to nuclear genes in the *Drosophila yakuba* species group. *Evolution.* 60:292–302.
- Barrett RD, Schluter D. 2008. Adaptation from standing genetic variation. *Trends Ecol. Evol. (Amst.)*. 23:38–44.
- Bolstad BM, Irizarry RA, Astrand M, Speed TP. 2003. A comparison of normalization methods for high density oligonucleotide array data based on variance and bias. *Bioinformatics.* 19:185–193.
- Cardoso-Moreira M, Arguello JR, Clark AG. 2012. Mutation spectrum of *Drosophila* CNVs revealed by breakpoint sequencing. *Genome Biol.* 13:R119.
- Cardoso-Moreira M, Emerson JJ, Clark AG, Long M. 2011. *Drosophila* duplication hotspots are associated with late-replicating regions of the genome. *PLoS Genet.* 7:e1002340.
- Chaisson MJ, Tesler G. 2012. Mapping single molecule sequencing reads using basic local alignment with successive refinement (BLASR): application and theory. *BMC Bioinformatics.* 13:238.

- Charlesworth B. 2012. The role of background selection in shaping patterns of molecular evolution and variation: evidence from variability on the *Drosophila* X chromosome. *Genetics*. 191:233–246.
- Charlesworth B, Coyne J, Barton N. 1987. The relative rates of evolution of sex chromosomes and autosomes. *American Naturalist*. pp. 113–146.
- Conant GC, Wolfe KH. 2008. Turning a hobby into a job: how duplicated genes find new functions. *Nat. Rev. Genet.* 9:938–950.
- Conrad DF, Pinto D, Redon R, et al. (28 co-authors). 2010. Origins and functional impact of copy number variation in the human genome. *Nature*. 464:704–712.
- Corbett-Detig RB, Cardeno C, Langley CH. 2012. Sequence-based detection and breakpoint assembly of polymorphic inversions. *Genetics*. 192:131–137.
- Cridland JM, Macdonald SJ, Long AD, Thornton KR. 2013. Abundance and distribution of transposable elements in two *Drosophila* QTL mapping resources. *Mol. Biol. Evol.* 30:2311–2327.
- Cridland JM, Thornton KR. 2010. Validation of rearrangement break points identified by paired-end sequencing in natural populations of *Drosophila melanogaster*. *Genome Biol Evol.* 2:83–101.
- Adams et al. 2000. The genome sequence of *Drosophila melanogaster*. *Science*. 287:2185–2195.
- Dopman EB, Hartl DL. 2007. A portrait of copy-number polymorphism in *Drosophila melanogaster*. *Proc. Natl. Acad. Sci. U.S.A.* 104:19920–19925.
- Drosophila Twelve Genomes Consortium. 2007. Evolution of genes and genomes on the *Drosophila* phylogeny. *Nature*. 450:203–218.
- Emerson JJ, Cardoso-Moreira M, Borevitz JO, Long M. 2008. Natural selection shapes genome-wide patterns of copy-number polymorphism in *Drosophila melanogaster*. *Science*. 320:1629–1631.
- Ewing B, Green P. 1998. Base-calling of automated sequencer traces using phred. II. Error probabilities. *Genome Res.* 8:186–194.
- Eyre-Walker A, Keightley PD, Smith NG, Gaffney D. 2002. Quantifying the slightly deleterious mutation model of molecular evolution. *Mol. Biol. Evol.* 19:2142–2149.
- Haddrill PR, Bachtrog D, Andolfatto P. 2008. Positive and negative selection on noncoding DNA in *Drosophila simulans*. *Mol. Biol. Evol.* 25:1825–1834.
- Hahn MW, Han MV, Han SG. 2007. Gene family evolution across 12 *Drosophila* genomes. *PLoS Genetics*. 3:e197.

- Harris RS. 2007. Improved pairwise alignment of genomic DNA. Ph.D. thesis, The Pennsylvania State University.
- Hu TT, Eisen MB, Thornton KR, Andolfatto P. 2012. A second generation assembly of the *Drosophila simulans* genome provides new insights into patterns of lineage-specific divergence. *Genome Res.* .
- Hu X, Worton RG. 1992. Partial gene duplication as a cause of human disease. *Hum. Mutat.* 1:3–12.
- Huddleston J, Ranade S, Malig M, et al. (14 co-authors). 2014. Reconstructing complex regions of genomes using long-read sequencing technology. *Genome Res.* .
- Inaki K, Liu ET. 2012. Structural mutations in cancer: mechanistic and functional insights. *Trends Genet.* 28:550–559.
- Ionita-Laza I, Rogers AJ, Lange C, Raby BA, Lee C. 2009. Genetic association analysis of copy-number variation (CNV) in human disease pathogenesis. *Genomics.* 93:22–26.
- Jones CD, Begun DJ. 2005. Parallel evolution of chimeric fusion genes. *Proceedings of the National Academy of Sciences, USA.* 102:11373–11378.
- Jones CD, Custer AW, Begun DJ. 2005. Origin and evolution of a chimeric fusion gene in *Drosophila subobscura*, *D. madeirensis* and *D. guanche*. *Genetics.* 170:207–219.
- Kearney HM, Kirkpatrick DT, Gerton JL, Petes TD. 2001. Meiotic recombination involving heterozygous large insertions in *Saccharomyces cerevisiae*: formation and repair of large, unpaired DNA loops. *Genetics.* 158:1457–1476.
- Kent WJ, Baertsch R, Hinrichs A, Miller W, Haussler D. 2003. Evolution’s cauldron: duplication, deletion, and rearrangement in the mouse and human genomes. *Proc Natl Acad Sci USA.* 100:11484–9.
- Korbel JO, Urban AE, Affourtit JP, et al. (23 co-authors). 2007. Paired-end mapping reveals extensive structural variation in the human genome. *Science.* 318:420–426.
- Lazarro B, Clark A. 2012. Rapidly Evolving Genes and Genetic Systems, chapter Rapid evolution of innate immune response genes. In: R.S. Singh and Kulathinal (2012).
- Lee YC, Reinhardt JA. 2012. Widespread polymorphism in the positions of stop codons in *Drosophila melanogaster*. *Genome Biol Evol.* 4:533–549.
- Li H, Durbin R. 2009. Fast and accurate short read alignment with Burrows-Wheeler transform. *Bioinformatics.* 25:1754–1760.
- Li H, Handsaker B, Wysoker A, Fennell T, Ruan J, Homer N, Marth G, Abecasis G, Durbin R. 2009. The Sequence Alignment/Map format and SAMtools. *Bioinformatics.* 25:2078–2079.

- Liang Q, Conte N, Skarnes WC, Bradley A. 2008. Extensive genomic copy number variation in embryonic stem cells. *Proc. Natl. Acad. Sci. U.S.A.* 105:17453–17456.
- Lim JK, Simmons MJ. 1994. Gross chromosome rearrangements mediated by transposable elements in *Drosophila melanogaster*. *Bioessays*. 16:269–275.
- Long M, Langley CH. 1993. Natural selection and the origin of *jingwei*, a chimeric processed functional gene in *Drosophila*. *Science*. 260:91–95.
- Mackay TF, Richards S, Stone EA, et al. (52 co-authors). 2012. The *Drosophila melanogaster* Genetic Reference Panel. *Nature*. 482:173–178.
- Mills RE, Walter K, Stewart C, Handsaker RE, Chen ea K. 2011. Mapping copy number variation by population-scale genome sequencing. *Nature*. 470:59–65.
- Ohshima K, Igarashi K. 2010. Inference for the initial stage of domain shuffling: tracing the evolutionary fate of the *PIPSL* retrogene in hominoids. *Molecular Biology and Evolution*. 27:2522–2533.
- Petrov DA, Lozovskaya ER, Hartl DL. 1996. High intrinsic rate of DNA loss in *Drosophila*. *Nature*. 384:346–349.
- Presgraves DC. 2008. Sex chromosomes and speciation in *Drosophila*. *Trends Genet.* 24:336–343.
- Ranz JM, Castillo-Davis CI, Meiklejohn CD, Hartl DL. 2003. Sex-dependent gene expression and evolution of the *Drosophila* transcriptome. *Science*. 300:1742–1745.
- Rogers RL, Bedford T, Hartl DL. 2009. Formation and longevity of chimeric and duplicate genes in *Drosophila melanogaster*. *Genetics*. 181:313–322.
- Rogers RL, Hartl DL. 2012. Chimeric genes as a source of rapid evolution in *Drosophila melanogaster*. *Mol. Biol. Evol.* 29:517–529.
- RS Singh JX, Kulathinal R, editors. 2012. *Rapidly Evolving Genes and Genetic Systems*. Oxford: Oxford University Press.
- Sawyer SA, Hartl DL. 1992. Population genetics of polymorphism and divergence. *Genetics*. 132:1161–1176.
- Schrider DR, Houle D, Lynch M, Hahn MW. 2013. Rates and genomic consequences of spontaneous mutational events in *Drosophila melanogaster*. *Genetics*. 194:937–954.
- Sudmant PH, Kitzman JO, Antonacci F, Alkan C, Malig ea M. 2010. Diversity of human copy number variation and multicopy genes. *Science*. 330:641–646.
- Tuzun E, Sharp AJ, Bailey JA, et al. (12 co-authors). 2005. Fine-scale structural variation of the human genome. *Nat. Genet.* 37:727–732.

- Viterbi A. 1967. Error bounds for convolutional codes and an asymptotically optimum decoding algorithm. *IEEE Transactions on Information Theory*. IT-13:260–269.
- Wong A, Wolfner M. 2012. Rapidly Evolving Genes and Genetic Systems, chapter Evolution of *Drosophila* seminal proteins and their networks. In: R.S. Singh and Kulathinal (2012).
- Wright S. 1931. Evolution in Mendelian Populations. *Genetics*. 16:97–159.
- Xie C, Tammi MT. 2009. CNV-seq, a new method to detect copy number variation using high-throughput sequencing. *BMC Bioinformatics*. 10:80.
- Ye K, Schulz MH, Long Q, Apweiler R, Ning Z. 2009. Pindel: a pattern growth approach to detect break points of large deletions and medium sized insertions from paired-end short reads. *Bioinformatics*. 25:2865–2871.
- Zhang J, Dean AM, Brunet F, Long M. 2004. Evolving protein functional diversity in new genes of *Drosophila*. *Proceedings of the National Academy of Sciences, USA*. 101:16246–16250.
- Zhang Y, Lu S, Zhao S, Zheng X, Long M, Wei L. 2009. Positive selection for the male functionality of a co-retroposed gene in the hominoids. *BMC evolutionary biology*. 9:252.
- Zhou Q, Zhang G, Zhang Y, Xu S, Zhao R, Zhan Z, Li X, Ding Y, Yang S, Wang W. 2008. On the origin of new genes in *Drosophila*. *Genome Research*. 18:1446–1455.
- Zichner T, Garfield DA, Rausch T, Stutz AM, Cannavo E, Braun M, Furlong EE, Korb JO. 2013. Impact of genomic structural variation in *Drosophila melanogaster* based on population-scale sequencing. *Genome Res*. 23:568–579.

Table S1: Sequencing statistics for *Drosophila yakuba* libraries

Species	Sample	Read length	Number of read pairs
<i>Drosophila yakuba</i>	reference	54	27,771,582
		76	29,065,488
		105	68,660,482
	CY20A	76	86,628,715
		76	35,886,204
		76	39,262,696
	CY28	54	31,908,008
		76	40,631,850
		76	33,242,246
	CY01A	48	25,239,444
		54	25,206,710
		76	25,393,295
	CY02B5	76	111,535,323
		48	20,266,663
		54	23,669,407
	CY04B	76	30,960,740
		48	20,525,873
		54	19,048,177
	CY08A	76	29,088,850
		76	81,634,715
		48	22,518,030
	CY13A	76	28,321,290
		54	31,630,793
		48	21,632,572
	CY17C	76	26,933,913
		54	31,252,102
		48	25,560,116
	CY21B3	76	30,498,100
		54	29,303,889
		76	116,502,064
	CY22B	48	21,084,747
		76	28,094,292
		54	24,831,622
	NY66-2	76	92,234,832
		54	21,924,434
		76	25,916,918
	NY81	54	26,611,105
		54	24,894,912
		76	26,776,198
	NY48	76	88,481,425
		54	25,534,953
		76	27,838,117
	NY56	76	85,887,835
		54	23,129,714
		76	28,500,212
	NY62	76	30,114,197
		54	26,486,845
		76	31,506,258
	NY65	76	32,601,617
		54	29,743,963
		76	30,946,111
	NY73	76	31,529,718
		54	27,490,843
		76	32,600,073
	NY42	76	28,468,446
		54	27,534,698
		76	31,988,717
NY85	76	29,556,013	
	54	33,715,271	
	76	42,770,174	
NY141	76	35,701,540	
	54	27,811,873	
	76	32,528,787	
16	76	33,047,656	
	54	25,298,106	
	76	80,761,937	
		76	30,145,168

CY= Cameroon *D. yakuba*, NY = Nairobi *D. yakuba*

Table S2: Sequencing statistics for *D. simulans* libraries

Species	Sample	Read length	Number of read pairs
<i>Drosophila simulans</i>	reference (<i>w501</i>)	104	46,855,159
	MD221	76	41,341,930
		76	43,274,500
	MD06	54	42,866,171
		54	40,300,257
		76	36,879,386
	MD63	76	44,594,779
		54	29,033,259
		76	34,548,640
	MD251	76	32,326,841
		76	42,795,040
		54	42,248,728
	MD105	76	43,250,191
		54	28,957,390
		76	35,059,033
	MD199	76	30,862,150
		54	39,280,145
		76	41,798,120
	MD106	76	42,708,601
		76	45,264,776
		76	45,425,267
	MD73	54	42,630,510
		76	43,929,651
		76	44,473,268
	MD15	76	24,882,026
		76	38,422,860
		76	38,035,776
	MD233	76	44,330,417
		76	38,302,627
		76	38,525,975
	NS40	54	41,655,021
		76	42,810,725
		76	44,451,089
	NS05	54	43,132,030
		76	42,000,020
		76	43,987,326
	NS137	54	31,917,670
		76	39,650,018
		76	34,951,602
	NS39	54	41,063,490
		76	42,341,695
		76	45,140,717
	NS67	76	42,962,176
		76	36,357,328
		76	39,932,110
	NS50	76	40,491,844
		76	32,795,824
		76	37,809,667
	NS113	76	37,031,543
		76	34,325,117
		76	37,031,994
	NS78	76	41,381,084
		76	36,771,570
		76	38,763,692
NS33	76	37,225,499	
	76	34,271,146	
	76	36,656,786	
NS79	76	38,326,489	
	76	36,965,044	
	76	40,146,925	

MD = Madagascar *D. simulans*, NS = Nairobi *D. simulans*.

Table S3: Bases with coverage in reference

chrom	<i>D. simulans</i>	<i>D. yakuba</i>
2L	23275275	28575774
2R	21329557	23894902
3L	23878518	21033386
3R	26966593	22193704
4	1007160	1342752
X	20607623	21512027

Table S4: Summaries of raw sequence coverage for inbred lines at mapping quality thresholds

Species	Sample	M_0^a	$f_{0,0}^b$	$Q_{1,0}^c$	M_{20}^a	$f_{0,20}^b$	$Q_{1,20}^c$	M_{30}^a	$f_{0,30}^b$	$Q_{1,30}^c$
<i>Drosophila simulans</i>	reference	55	0.012	8	55	0.046	15	49	0.047	10
	MD221	118	0.017	19	116	0.051	25	90	0.071	5
	MD06	115	0.017	17	113	0.051	24	85	0.071	4
	MD63	90	0.017	15	89	0.051	22	70	0.071	3
	NS40	121	0.017	22	119	0.051	32	95	0.070	5
	MD251	118	0.017	19	116	0.051	26	90	0.071	5
	MD105	92	0.016	14	90	0.051	22	71	0.070	3
	MD199	114	0.017	19	112	0.051	27	90	0.069	5
	NS05	119	0.017	20	118	0.051	27	92	0.069	5
	NS137	98	0.017	17	96	0.051	26	76	0.071	4
	NS39	121	0.016	20	119	0.051	30	94	0.069	5
	MD73	120	0.016	20	118	0.051	29	93	0.069	5
	MD106	87	0.018	14	86	0.052	18	64	0.078	4
	NS67	124	0.018	21	122	0.051	34	97	0.075	6
	NS50	117	0.017	19	116	0.052	29	91	0.076	6
	NS113	111	0.017	18	109	0.051	27	85	0.074	5
	NS78	122	0.018	19	120	0.051	25	94	0.075	6
	MD15	97	0.018	16	95	0.052	21	71	0.078	4
	NS33	111	0.017	18	109	0.051	26	86	0.074	5
	NS79	120	0.018	21	118	0.051	29	93	0.075	6
MD233	121	0.017	21	119	0.051	30	90	0.076	5	
<i>Drosophila yakuba</i>	reference	124	0.009	36	122	0.015	11	111	0.023	4
	CY20A	149	0.013	20	146	0.032	4	121	0.060	3
	CY28	85	0.013	11	83	0.036	3	66	0.067	2
	CY01A	151	0.012	21	148	0.032	4	123	0.056	2
	CY02B5	55	0.013	8	54	0.039	2	44	0.067	2
	CY04B	125	0.013	17	123	0.036	4	102	0.063	2
	CY08A	57	0.013	9	55	0.036	2	45	0.066	1
	CY13A	56	0.014	9	54	0.036	2	45	0.068	1
	CY17C	151	0.012	21	148	0.031	4	118	0.058	2
	CY21B3	139	0.012	21	137	0.029	3	113	0.053	2
	CY22B	56	0.014	8	55	0.038	2	45	0.071	1
	NY66-2	110	0.014	15	107	0.038	4	85	0.070	2
	NY81	107	0.014	14	104	0.038	5	82	0.070	2
	NY48	64	0.015	9	62	0.040	3	49	0.072	2
	NY56	60	0.016	7	58	0.044	4	45	0.081	2
	NY62	70	0.013	10	68	0.036	3	54	0.066	2
	NY65	69	0.014	10	68	0.039	4	54	0.072	2
	NY73	68	0.015	9	66	0.041	4	53	0.073	2
	NY42	93	0.014	12	91	0.037	3	74	0.067	2
	NY85	79	0.013	12	78	0.033	3	64	0.062	2
NY141	110	0.015	14	108	0.041	6	87	0.073	3	

^a M_X refers to median coverage of major chromosome arms at mapping quality $\geq X$.

^b $f_{0,X}$ refers to the fraction of the major arms with coverage of zero at mapping quality $\geq X$.

^c $Q_{1,X}$ refers to the first quantile of sites with coverage ≥ 0 and mapping quality $\geq X$. In other words, 99% of sites with coverage ≥ 0 have coverage $\leq Q_{1,X}$.

Table S5: Summary statistics of library insert sizes.

Species	Sample ^a	Median fragment size	99.9 th quantile of fragment sizes
<i>Drosophila simulans</i>	reference (<i>w501</i>)	532	593 ^b
	MD221	318	527
	MD06	319	551
	MD63	302	636
	MD251	325	580
	MD105	316	702
	MD199	344	584
	MD73	317	537
	MD106	319	529
	MD233	301	501
	MD15	313	511
	NS40	316	602
	NS05	324	558
	NS137	317	647
	NS39	318	549
	NS67	314	517
	NS50	330	571
	NS113	334	581
	NS78	326	550
	NS33	327	543
NS79	332	562	
<i>Drosophila yakuba</i>	reference	343	565
	CY20A	336	998
	CY28	308	1,018
	CY01A	322	1,124
	CY02B5	313	1,183
	CY04B	327	1,123
	CY08A	322	1,338
	CY13A	316	1,070
	CY17C	338	1,102
	CY21B3	372	1,226
	CY22B	328	1,156
	NY66-2	313	989
	NY81	326	1,063
	NY48	322	1,030
	NY56	332	1,069
	NY62	319	1,037
	NY65	341	1,089
	NY73	325	1,078
	NY42	270	725
	NY85	326	1,036
NY141	336	1,061	

^a MD = Madagascar *D. simulans*, NS = Nairobi *D. simulans*, CY = Cameroon *D. yakuba*, and NY = Nairobi *D. yakuba*.

^b For this sample, the actual value calculated from alignments was $> 10^6$. The value we used, which is shown in the table, is the mean value for the non-reference samples.

Table S6: Number of tandem duplications in sample strains.

Species	Strain	Duplications
	CY20A	145
	CY28	160
	CY01A	207
	CY02B5	179
	CY04B	154
	CY08A	184
	CY13A	159
	CY17C	230
	CY21B3	224
	CY22B	136
	NY66-2	134
	NY81	126
	NY48	106
	NY56	81
	NY62	154
	NY65	107
	NY73	100
	NY42	138
	NY85	169
	NY141	121
	std	40.22
	mean	151.0
	median	154.0
<i>D. simulans</i>	MD221	119
	MD06	117
	MD63	122
	NS40	119
	MD251	110
	MD105	130
	MD199	100
	NS05	160
	NS137	107
	NS39	129
	MD73	102
	MD106	85
	NS67	120
	NS50	109
	NS113	113
	NS78	113
	MD15	93
	NS33	111
	NS79	117
	MD233	102
	std	15.56
	Mean	113.63
	Median	113.0

Table S7: Number of tandem duplications in sample and reference strains.

Species	Strain	Duplications
<i>D. yakuba</i>	reference	38
	CY20A	154
	CY28	170
	CY01A	225
	CY025B	187
	CY04B	172
	CY08A	201
	CY13A	168
	CY17C	248
	CY21B3	247
	CY22B	148
	NY66-2	151
	NY81	135
	NY48	107
	NY56	81
	NY62	166
	NY65	114
	NY73	114
	NY42	152
	NY85	182
NY141	128	
	mean	162.5
	median	160
	stdev	43.53
<i>D. simulans</i>	w^{501}	93
	MD221	171
	MD06	169
	MD63	180
	MD251	174
	MD105	195
	MD199	159
	MD73	165
	MD106	136
	MD15	141
	NS40	174
	NS05	219
	NS137	165
	NS39	187
	NS67	172
	NS50	164
	NS113	161
	NS78	166
	NS33	166
	NS79	170
MD233	156	
	mean	165.86
	median	166
	stdev	23.44

Table S8: PacBio Confirmation

Line	Chromosome	Total	Confirmed
CY17C	2L	41	40
	2R	70	69
	3L	38	36
	3R	30	25
	X	48	46
	4	3	3
CY21B3	2L	53	43
	2R	57	55
	3L	34	34
	3R	36	36
	X	43	43
	4	1	1
NY66-2	2L	28	26
	2R	30	29
	3L	17	16
	3R	24	22
	X	33	33
	4	2	2
NY73	2L	19	16
	2R	24	23
	3L	21	20
	3R	15	14
	X	21	18
	4	0	0

Table S9: Fraction of genome covered in 3 or more reads in downsampled sequences of line CY17C

Median coverage	Fraction Covered
15X	0.866
30X	0.898
45X	0.909
60X	0.914
75X	0.92
90X	0.92
105X	0.923
120X	0.923
135X	0.926
150X	0.928

Table S10: P -value for Fisher's Exact Test of PCR confirmation rates

Study	Confirmed	Total	<i>D. simulans</i>	<i>D. yakuba</i>
Emerson et al. 2008	64	74	0.7855	2.089×10^{-5}
Cridland et al 2010	75	78	0.0319	1.642×10^{-9}
Cardoso et al. 2011	18	24	0.5230	0.0725
Cardoso et al. 2012	32	32	0.0169	3.4194×10^{-7}
Zichner et al. 2013	22	23	0.2422	1.1579×10^{-4}
Schrider et al. 2013	7	19	0.0007	0.4165

Table S11: PacBio Sequencing Reads

Line	Cell	Avg Length	Min Length	Max Length	Total Reads
CY17C	1	2424	50	21696	137839
CY17C	2	2418	50	21680	134568
CY17C	3	2175	50	19084	103354
CY17C	4	2161	50	20519	112597
CY17C	5	2148	50	18949	118144
CY21B3	1	2571	50	24042	123592
CY21B3	2	2549	50	22398	129855
CY21B3	3	2224	50	22206	161532
CY21B3	4	2152	50	20779	15733
CY21B3	5	2060	50	18204	149234
NY66-2	1	2556	50	22178	150291
NY66-2	2	2485	50	21204	112095
NY66-2	3	2648	50	21161	139571
NY66-2	4	2059	50	20709	184485
NY66-2	5	2699	50	22203	149048
NY73	1	2269	50	17924	95028
NY73	2	2200	50	17927	92587
NY73	3	2175	50	17779	97116
NY73	4	2137	50	19110	83372
NY73	5	2175	50	19084	87212

Table S12: Direct repeats 300bp or larger within 25kb span in reference

Species	Chrom	Number
<i>D. yakuba</i>	2L	13
	2R	10
	3L	41
	3R	43
	X	13
<i>D. simulans</i>	2L	2
	2R	0
	3L	3
	3R	0
	X	0

Table S13: Overrepresented GO categories among duplicated genes at EASE ≥ 1.0

Species	Functional Category	Group EASE score
<i>D. yakuba</i>	Alternative splicing	3.54
	Immunoglobulin and Fibronectin	2.70
	Chitins and aminoglycans	2.00
	Signal peptide or glycoprotein	1.54
	Immune response to wound healing	1.44
	Drug and hormone metabolism	1.37
	Extracellular matrix	1.34
	Immune response to pathogens	1.17
	Neurodevelopment and morphogenesis	1.17
	Chemotaxis	1.12
	Chorion Development	1.07
<i>D. simulans</i>	Oxidation-reduction and secondary metabolites	2.63
	Cytochromes, oxidoreductases, and toxin metabolism	2.32
	Lipases	1.61
	Immune response to bacteria	1.59
	phospholipid metabolism	1.45
	Chemosensory processing	1.37
	Gultathion transferase and drug metabolism	1.21
	Carboxylesterases	1.2
	Sarcomeres	1.0
	Cuticle development	0.97
	Endopeptidases	0.87

Table S14: Overrepresented GO categories in independently duplicated genes

Multiple Independent Duplications		
<i>D. yakuba</i>	Chorion Development and oogenesis	1.79
	Cell signaling	1.34
	Sensory processing	1.23
	Immune response	1.11
	Development	1.05
<i>D. simulans</i>	Immune Response to Bacteria	3.35
	Chorion Development and oogenesis	1.84
	Organic Cation Membrane Transport	1.48
	Chemosensory Perception	1.41

Table S15: Gene Duplications Identified at a Sample Frequency $\geq \frac{17}{20}$

Species	Chrom	Start	Stop	Genes	Ontologies
<i>D. yakuba</i>	2L	20867709	20868709	<i>GE19441</i>	cation transport
	2L	4561989	4563943	<i>GE14706</i>	Epidermal growth factor; Follistatin-like; Zona pellucida
	2R	1192252	1198186	<i>GE12923</i>	Adenyl cyclase
	2R	8627195	8631730	<i>GE13451, GE13452</i>	AMP dependent ligases or synthetases
	2R	9718894	9722579	<i>GE12353, GE12354, GE13533</i>	serine-type endopeptidases
	2L	22229672	22240590	-	-
	2R	2456185	2468412	-	-
	2R	550564	555698	-	-
	X	2263061	2263383	-	-
	X	6027171	6028326	-	-
	3L	6853202	6857398	-	-
	3L	1631349	1632283	-	-
	3R	28797150	28798631	-	-
<i>D. simulans</i>	2L	15442908	15460870	<i>CG7653</i>	aminopeptidase; male reproduction
	2R	19220441	19221209	<i>CG3510</i>	mitotic spindle movement and cytokinesis
	2R	6705454	6706432	<i>CG18445</i>	cellular calcium homeostasis, adult lifespan
	3L	1138079	1141222	<i>CG1179</i>	antimicrobial response
	3L	1138061	1151515	<i>CG9116, CG1165, CG1180, CG1179</i>	antimicrobial response
	3R	12694264	12697515	<i>CG11600, CG11598, CG11608</i>	lipase; accessory gland
	X	10711505	10714527	<i>CG1725</i>	development and morphogenesis
	X	815864	816572	<i>CG11638</i>	EF-hand-like domain
	X	3859088	3860485	<i>CG12691</i>	no data
	X	4216151	4218438	<i>CG12179, CG12184</i>	no data
	2L	22881359	22884258	-	-
	2R	1782843	1783435	-	-
	2R	1849682	1858187	-	-
	2R	368797	369174	-	-
	2R	6769473	6770112	-	-
	3L	16974345	16975592	-	-
	3L	23132385	23145527	-	-
	3L	23499705	23500091	-	-
	X	10810038	10810658	-	-
	X	14784709	14784963	-	-
	X	1942550	1943315	-	-
	X	20173558	20177752	-	-
	X	3953557	3954555	-	-
	X	4353206	4354968	-	-
	X	7149884	7152082	-	-

Table S16: Recruited Non-Coding Sequence in *D. yakuba* I

Type	Gene	Chrom	Start	Stop	Strand	Strains
Recruited Non-Coding	GE18269	2L	4024479	4026346	+	1
	GE11906	2R	15447621	15450093	-	1
	GE13954	2R	15422288	15424931	+	1
	GE10773	2L	11412985	11416198	-	1
	GE12793	2R	3641829	3654689	-	1
	GE20665	3L	4498924	4499419	-	1
	GE20642	3L	4748069	4750627	-	1
	GE12985	2R	1220523	1223522	+	3
	GE25403	3R	456693	474667	+	3
	GE14641	2L	5056039	5058911	-	1
	GE24887	3R	7559447	7567609	-	1
	GE18834	2L	12012286	12013371	+	1
	GE14103	2R	17064455	17068625	+	1
	GE14204	2R	18340872	18341767	+	6
	GE19947	3L	15944998	15948170	-	2
	GE13585	2R	10199336	10208268	+	1
	GE17610	X	15169824	15171000	+	1
	GE13833	2R	13593056	13597666	+	1
	GE12921	2R	1296122	1299376	-	4
	GE22103	3L	16172247	16172603	+	2
	GE20019	3L	14602982	14605035	-	1
	GE13348	2R	7486324	7489683	+	1
	GE23504	3R	26016459	26016872	-	2
	GE26314	3R	14152097	14152483	+	1
	GE17862	X	19312815	19315826	+	1
	GE12906	2R	1569408	1572051	-	1
	GE24569	3R	12091442	12096476	-	1
	GE23710	3R	23607275	23608177	-	1
	GE19620	3L	20846937	20859977	-	1
	GE14485	4	1300833	1304379	-	1
	GE24349	3R	14703209	14705506	-	1
	GE23444	3R	26616440	26618338	-	1
	GE12929	2R	921000	926017	-	1
	GE14093	2R	16915401	16922730	+	1
	GE18272	2L	4137997	4143127	+	1
	GE16590	X	157495	158134	-	1
	GE18174	2L	2726172	2731718	+	1
	GE13324	2R	7085103	7088180	+	1
	GE19465	2L	22202637	22205208	+	1
	GE23519	2L	16475111	16476986	-	1
	GE21452	3L	5038513	5043130	+	1
	GE13128	2R	3600589	3603993	+	1
	GE19410	2L	20057880	20060145	+	1
	GE11423	2R	20547562	20548621	-	1
	GE24770	3R	9392640	9392863	-	4
	GE20162	3L	11976337	11979310	-	1
	GE25302	3R	1445612	1450376	-	1
	GE21054	3L	115270	118715	+	1

Table S17: Recruited Non-Coding Sequence in *D. yakuba* II

Type	Gene	Chrom	Start	Stop	Strand	Strains
Recruited Non-Coding	GE16460	2L	108667	108970	-	1
	GE13445	2R	8579441	8581528	+	2
	GE13294	2R	6537075	6541877	+	1
	GE18814	2L	11619990	11635209	+	1
	GE18468	2L	6924773	6926435	+	1
	GE18653	2L	9824910	9828235	+	1
	GE12963	2R	363102	367650	+	2
	GE21059	3L	156476	159503	+	1
	GE19269	2L	17827409	17829872	+	1
	GE26141	2L	12979610	12983013	-	1
	GE19225	2L	17288040	17288648	+	1
	GE21286	3L	3185710	3196869	+	2
	GE10233	3R	18382396	18384823	+	6
	GE12947	2R	392470	401311	-	1
	GE19172	2L	16627714	16628834	+	1
	GE13092	2R	2741691	2741955	+	1
	GE24207	3R	16710156	16712312	-	1
	GE14560	4	808540	816641	+	1
	GE18453	2L	6552459	6556843	+	1
	GE11989	2L	9417833	9419230	-	1
	GE12986	2R	1265746	1283900	+	1
	GE14704	2L	4595905	4603145	-	1
	GE10115	2L	12647621	12647846	-	1
	GE21984	2L	18369608	18370669	-	1
	GE12947	2R	385328	401500	-	1
	GE13641	2R	11060164	11061595	+	2
	GE23918	3R	20559041	20560656	-	2
	GE24208	3R	16678984	16680305	-	1
	GE13389	2R	7860267	7865453	+	1
	GE15418	X	18564946	18568426	-	1
	GE17176	X	9412662	9415570	+	1
	GE21334	3L	3723736	3727362	+	1
	GE26071	3R	11008671	11012107	+	2
	GE16233	X	6345642	6350148	-	1
	GE10260	3R	18673427	18675156	+	1
	GE15086	2L	2556400	2557925	-	1
	GE14314	2R	19547242	19551254	+	1
	GE14531	4	41861	42853	-	1
	GE17162	X	9152733	9154332	+	1
	GE19996	3L	15023729	15026407	-	5
	GE25401	3R	444738	446198	+	1
	GE10771	3R	25846233	25849137	+	1
	GE18000	3L	18980225	18991194	-	3
GE12947	2R	385387	401772	-	1	
GE15364	X	19336095	19338151	-	1	
GE13453	2R	8628288	8637097	+	6	

Table S18: Recruited Non-Coding Sequence in *D. simulans* I

Type	Gene	Chrom	Start	Stop	Strand	Strains
Recruited Non-Coding	CG5939	3L	8520531	8500705	-	1
	CG3955	2R	9687651	9686889	-	2
	CG30030	2R	7961858	7960689	+	1
	CG5925	3R	12851812	12842698	-	1
	CG3823	X	5828413	5826778	+	1
	CG15252	X	9410423	9407893	-	1
	CG12487	3L	14581107	14579140	-	8
	CG4004	X	11999000	11996338	+	2
	CG3919	3L	14069074	14065733	+	1
	CG9692	3L	16291819	16289912	+	1
	CG7058	X	17623953	17619037	+	1
	CG8859	2R	8781970	8776750	-	2
	CG10251	3R	19075153	19071626	-	1
	CG5685	3R	4469843	4462120	-	1
	CG31536	3R	697054	692538	+	1
	CG12691	X	3860485	3859088	+	18
	CG5659	X	17126212	17124294	-	1
	CG7678	3R	7067181	7063437	+	1
	CG18063	2L	15538184	15535240	+	2
	CG9431	2L	12835101	12832723	-	1
	CG4572	3R	5597362	5594122	+	1
	CG31450	3R	16589187	16588657	+	1
	CG2174	X	10322987	10304124	+	1
	CG6134	3R	22342992	22341162	-	1
	CG3210	2L	2472529	2463036	-	1
	CG6308	X	14530096	14528791	+	1
	CG1851	2R	3965243	3961574	-	1
	CG3208	X	5145948	5145204	-	6
	CG13350	2R	10556652	10549764	-	4
	CG3647	2L	14671041	14666003	+	1
	CG7914	X	17986800	17986419	-	1
	CG6643	3R	19913528	19912399	+	2
	CG6416	3L	8421994	8418765	+	1
	CG17446	X	8714153	8711653	-	1
	CG3558	2L	2878467	2874676	+	1
	CG5939	3L	8521640	8500872	-	1
	CG10240	2R	11466660	11464170	+	1
	CG17927	2L	16357771	16354240	+	1
	CG13658	3R	20627528	20624799	+	1
	CG14724	3R	13454925	13451797	-	1
	CG42575	3L	10870586	10866452	+	3
	CG9689	X	9313627	9312603	+	1
	CG12184	X	4215528	4213588	-	1
	CG1486	X	19933936	19931912	+	1
	CG17510	2R	2451922	2448224	-	2
	CG12065	X	8054167	8053646	+	1
	CG1179	3L	1141222	1138079	+	20
CG5939	3L	8520189	8500848	-	1	
CG32703	X	8703815	8700230	-	2	

Table S19: Recruited Non-Coding Sequence in *D. simulans* II

Type	Gene	Chrom	Start	Stop	Strand	Strains
Recruited Non-Coding	CG33223	X	7929354	7921199	-	6
	CG31705	2L	11219262	11213928	-	2
	CG4335	3R	5071920	5071599	+	1
	CG5939	3L	8522666	8500416	-	1
	CG9914	X	15320652	15317592	-	1
	CG40486	X	20790004	20788766	-	1
	CG6667	2L	16997487	16991856	-	1
	CG5772	2L	9867394	9858502	-	1
	CG5939	3L	8526072	8502756	-	1
	CG6680	3L	19904005	19895648	+	2
	CG17921	2R	18143092	18133788	-	1
	CG5939	3L	8521943	8500015	-	1
	CG31118	3R	20168765	20167250	-	15
	CG32452	3L	22218538	22215418	+	3
	CG6203	3R	15121661	15121183	+	1
	CG7398	3L	6104564	6098227	+	1
	CG31164	3R	17481879	17479404	+	1
	CG3726	X	5475457	5471459	+	4
	CG34454	3L	202674	199394	-	1
	CG9380	2R	21517959	21517361	-	1
	CG13225	2R	7858337	7855361	+	8
	CG6511	3L	8513193	8508493	+	1
	CG1165	3L	1142790	1141414	-	14
	CG5409	2R	13335070	13334296	+	1
	CG1925	2R	4531779	4527304	+	1
	CG11158	X	12915981	12913430	+	1
	CG1179	3L	1151515	1138061	+	20
	CG9126	X	14999000	14996974	-	1
	CG11030	2L	5566837	5563794	+	1
	CG13225	2R	7859420	7856642	+	2
	CG8887	3L	19234359	19234240	-	1
	CG11325	2L	6485615	6483354	-	1
	CG2174	X	10323004	10304482	+	4
	CG4026	2L	9474185	9468950	+	8
	CG4937	X	15950724	15945545	+	1
	CG5939	3L	8521697	8497398	-	1
	CG14803	X	1624945	1623645	+	1
	CG6231	3R	5832844	5822195	+	2
	CG33223	X	7930084	7921981	-	1
	CG2174	X	10323255	10302508	+	1
	CG10146	2R	11339645	11337864	+	2
	CG9331	2L	20280987	20279429	+	1
	CG5939	3L	8519186	8500624	-	1
	CG9761	3R	493871	486754	-	1
	CG4086	3L	16204452	16202997	-	1
	CG5939	3L	8519120	8497461	-	1
	CG30497	2R	4466546	4459504	-	1

Table S20: Putative Dual Promoter Genes in *D. yakuba*

Type	5' Gene	3' Gene	Chrom	Start	Stop	Strand	Strains
Dual Promoter	GE25749	GE24961	3R	6426573	6429128		1
	GE17248	GE15994	X	10111434	10113143		1
	GE25858	GE24866	3R	8159079	8162914		1
	GE21080	GE21031	3L	282949	286511		1
	GE10392	GE23928	3R	20485903	20487331		1
	GE19241	GE22696	2L	17479513	17482694		1
	GE10859	GE23415	3R	26875286	26881333		1
	GE26132	GE24588	3R	11912024	11916314		3
	GE17889	GE15249	2L	2014960	2019346		1
	GE14337	GE11513	2R	19768417	19770224		1
	GE16626	GE16372	2L	146434	147628		1
	GE13245	GE12657	2R	5880254	5883193		1
	GE14570	GE14484	4	1314161	1319175		1
	GE16771	GE16447	X	2623733	2628942		1
	GE14002	GE11855	2R	15989525	15990929		1
	GE13989	GE11866	2R	15777997	15781002		1
	GE25878	GE24850	3R	8267252	8270103		1
	GE10233	GE24091	3R	18383837	18386578		2
	GE18995	GE25461	2L	13658567	13660529		4
	GE13812	GE12098	2R	13042582	13049000		1
	GE13138	GE12791	2R	3686554	3691429		3
	GE21885	GE20148	3L	12173462	12175684		1
	GE17429	GE15699	2L	1162125	1162631		1
	GE19355	GE21644	2L	18836291	18841517		1
	GE14442	GE11414	2R	20628266	20630184		1
	GE13815	GE12096	2R	13052601	13054893		1
	GE17290	GE15947	X	10693772	10694086		2
	GE18487	GE13339	2L	7166837	7171789		1
	GE19240	GE22696	2L	17477743	17483758		3
	GE26291	GE24418	3R	13841865	13844988		1
	GE21597	GE20441	3L	7731981	7736528		1
	GE13211	GE12702	2R	5347302	5349788		2
	GE26230	GE24475	3R	13110215	13112850		1
	GE13929	GE11929	2R	15128544	15131155		1
	GE21085	GE21022	3L	343902	348093		1
	GE10951	GE23313	3R	28355223	28357215		1
	GE26060	GE24657	3R	10734970	10739334		1
	GE16619	GE16580	X	349074	349922		1
	GE13338	GE12567	2R	7221214	7224978		1
	GE25687	GE25035	3R	5444807	5445189		1

Table S21: Putative Dual Promoter Genes in *D. simulans* I

Type	5' Gene	3' Gene	Chrom	Start	Stop	Strand	Strains
Dual Promoter	CG4433	CG4845	3R	5438512	5436655		1
	CG10086	CG18748	3R	3506551	3501272		1
	CG12230	CG3917	X	18350597	18348732		1
	CG9506	CG9500	2L	6166401	6152814		1
	CG7034	CG5760	3R	4371721	4366499		1
	CG13472	CG5295	3L	14429033	14427393		1
	CG3423	CG9211	2L	6722948	6714828		1
	CG5588	CG5611	3R	22888188	22885586		1

Table S22: Putative Chimeric Genes in *D. yakuba* I

Type	5' Gene	3' Gene	Chrom	Start	Stop	Strand	Strains
Chimeric	GE18811	GE18814	2L	11624699	11635716	+	2
	GE12444	GE12447	2R	8682740	8684098	-	1
	GE12828	GE12831	2R	2621213	2625329	-	5
	GE21209	GE21211	3L	2196531	2199567	+	1
	GE16478	GE16479	X	2094815	2098815	-	1
	GE12441	GE12442	2R	8693878	8697950	-	16
	GE25203	GE25214	2L	14060529	14065910	-	1
	GE19619	GE19620	3L	20848448	20861465	-	1
	GE10625	GE10626	3R	24047193	24049829	+	1
	GE19343	GE19344	2L	18662414	18663086	+	1
	GE13385	GE13386	2R	7858807	7861090	+	2
	GE17209	GE17211	X	9829925	9831752	+	1
	GE19944	GE19947	3L	15944832	15946907	-	1
	GE12275	GE12276	2R	10705351	10711729	-	10
	GE16764	GE16765	X	2538959	2540881	+	3
	GE23781	GE23782	3R	22385664	22386968	-	2
	GE14304	GE14305	2R	19416793	19423595	+	1
	GE26358	GE26359	3R	14778214	14779539	+	1
	GE10773	GE10784	2L	11411312	11413493	-	1
	GE21046	GE21047	3L	153714	155228	-	1
	GE18427	GE18428	2L	6328720	6335333	+	1
	GE15774	GE15775	X	13146906	13148951	-	1
	GE13156	GE13157	2R	4244726	4248299	+	1
	GE13078	GE13079	2R	2529175	2532039	+	1
	GE18932	GE18933	2L	13058912	13060325	+	1
	GE18810	GE18812	2L	11616544	11627893	+	8
	GE15105	GE15108	2L	2406236	2408538	-	1
	GE23853	GE23854	3R	21163271	21166358	-	1
	GE26117	GE26119	3R	11563789	11567495	+	1
	GE12353	GE12354	2R	9718894	9722579	-	19
	GE19681	GE19682	3L	20114778	20124632	-	1
	GE21817	GE21818	3L	11535053	11537096	+	1
	GE25203	GE25214	2L	14060197	14065508	-	1
	GE21123	GE21125	3L	1172484	1179048	+	1
	GE10460	GE10461	3R	21424020	21428007	+	7
	GE12766	GE12767	2R	4305793	4310361	-	1
	GE10682	GE10684	3R	25036642	25044043	+	4
	GE14192	GE14193	2R	18131313	18134201	+	1
	GE20247	GE20248	3L	11082344	11085513	-	8
	GE14235	GE14236	2R	18687558	18689712	+	4
	GE24523	GE24524	3R	12546325	12548762	-	1
	GE12451	GE12452	2R	8660527	8664855	-	1
	GE14191	GE14192	2R	18127656	18131007	+	1
	GE26194	GE26195	3R	12581548	12584840	+	5
	GE13732	GE13734	2R	12089189	12095200	+	1
	GE15325	GE15326	X	20043093	20045334	-	1
	GE13428	GE13439	2L	7100699	7103913	-	1

Table S23: Putative Chimeric Genes in *D. yakuba* II

Type	Gene	Chrom	Start	Stop	Strand	Strains	
Chimeric	GE11692	GE11693	2R	17841057	17843909	-	4
	GE16094	GE16096	X	8950320	8954906	-	12
	GE10460	GE10461	3R	21423681	21427312	+	2
	GE23849	GE23860	2L	16088829	16091980	-	1
	GE10382	GE10383	3R	20409220	20411134	+	1
	GE21851	GE21854	3L	11841757	11854748	+	13
	GE23589	GE23592	3R	25372683	25379092	-	5
	GE19428	GE19429	2L	20518336	20525187	+	1
	GE12481	GE12482	2R	8432422	8439919	-	4
	GE16583	GE16584	X	303209	310866	-	1
	GE25989	GE25990	3R	9654460	9658865	+	1
	GE20212	GE20213	3L	11535513	11537526	-	1
	GE18810	GE18811	2L	11616597	11622870	+	1
	GE26258	GE26259	3R	13421611	13426161	+	1
	GE13653	GE13654	2R	11216791	11218480	+	1
	GE18474	GE18475	2L	7043543	7048586	+	5
	GE15105	GE15108	2L	2405167	2407381	-	3
	GE11452	GE11454	2R	20345528	20347724	-	2
	GE13618	GE13619	2R	10699218	10701733	+	8
	GE10109	GE10110	3R	17036248	17039632	+	1
	GE11708	GE11711	2R	17603369	17607091	-	1
	GE11640	GE11641	2R	18527790	18532538	-	1
	GE13733	GE13734	2R	12091221	12095128	+	7
	GE16141	GE16142	X	7932016	7934615	-	1
	GE22398	GE22399	3L	20111729	20121616	+	1
	GE21366	GE21367	3L	4011112	4013997	+	1
	GE18810	GE18814	2L	11616623	11633710	+	1
	GE18648	GE18649	2L	9807924	9808680	+	1
	GE18812	GE18814	2L	11628837	11634750	+	1
	GE18811	GE18812	2L	11623999	11627896	+	1
	GE25583	GE25584	3R	3641910	3644927	+	1

Table S24: Putative Chimeric Genes in *D. simulans*

Type	5' Gene	3' Gene	Chrom	Start	Stop	Strand	Strains
Chimeric	CG11608	CG11598	3R	12697515	12694264	-	20
	CG10243	CG10240	2R	11467239	11463409	+	1
	CG3523	CG3524	2L	2944012	2931797	+	6
	CG33162	CG5939	3L	8516515	8502674	-	2
	CG10958	CG2116	X	7600264	7599314	+	1
	CG6607	CG13618	3R	19885309	19882164	+	3
	CG17970	CG14032	2L	5075704	5069930	+	1
	CG32261	CG1134	3L	3915856	3910469	+	1
	CG15797	CG17754	X	8697294	8694573	+	1
	CG18330	CG1049	3L	1464803	1462282	+	2
	CG10246	CG10247	2R	11475068	11469403	-	1
	CG6533	CG6511	3L	8514363	8506572	+	1
	CG2071	CG1304	X	19554392	19552342	-	1
	CG4231	CG12193	2L	1461505	1459358	+	1
	CG33162	CG5939	3L	8517417	8502361	-	1
	CG33162	CG5939	3L	8519388	8502448	-	1
	CG18779	CG10534	3L	6035588	6032981	-	5
	CG13946	CG12506	2L	739495	736512	+	1
	CG13160	CG33012	2R	8966253	8961795	+	1
	CG4215	CG7480	2L	13945968	13940471	+	1
	CG32257	CG32261	3L	3917056	3916219	+	1
	CG2767	CG11052	3R	3721593	3720813	-	1
	CG33013	CG30043	2R	8957288	8953622	+	1
	CG32383	CG32382	3L	7299216	7297924	-	1
	CG32252	CG15009	3L	4185415	4182425	-	1
	CG17760	CG17759	2R	9222236	9218438	+	1
	CG4200	CG12223	X	15354878	15351613	+	1
	CG33162	CG5939	3L	8525442	8502118	-	1
	CG5196	CG34402	3R	12884563	12880752	-	1
	CG33115	CG8942	2L	13552279	13546280	-	7
	CG14935	CG14934	2L	11526363	11522417	+	1
	CG14987	CG1134	3L	3920390	3910549	+	3
	CG32751	CG32754	X	5729860	5725985	-	1
	CG33162	CG5939	3L	8526534	8501627	-	1
	CG32280	CG11495	3L	3024302	3020851	+	1
	CG4231	CG12193	2L	1460323	1458239	+	1
	CG6533	CG6511	3L	8514355	8507883	+	1
	CG4381	CG4181	3R	12913682	12912587	-	1

Table S25: Number of duplications and association with repetitive sequence by chromosome

Species	Chrom	Total	100bp Repeat	30bp Repeat	TE within 1kb	TE within 100bp
<i>D. yakuba</i>	2L	334	16	45	50	14
	2R	294	34	52	63	17
	3L	225	22	35	13	3
	3R	256	32	52	21	6
	X	279	18	50	17	7
	4	27	3	3	15	4
	Total	1415	125	237	179	52
<i>D. simulans</i>	2L	154	9	23	18	8
	2R	200	8	23	41	17
	3L	198	5	19	31	16
	3R	178	8	18	3	1
	X	231	26	67	25	9
	4	14	0	0	3	1
	Total	975	56	150	121	52

Table S26: Direct repeats 30bp or larger within 25kb span in reference

Species	Chrom	Number
<i>D. yakuba</i>	2L	117
	2R	94
	3L	80
	3R	154
	X	78
<i>D. simulans</i>	2L	62
	2R	48
	3L	25
	3R	46
	X	24

Table S27: Tukey's HSD test for log normalized duplication size by chromosome

Species	Chromosome	vs. Chromosome	Difference	Lower	Upper	Adjusted P -value
<i>D. yakuba</i>	2R	2L	0.399	0.092	0.706	$2.95 \times 10^{-3**}$
	3L	2L	-0.128	-0.459	0.204	0.881
	3L	2R	-0.527	-0.867	-0.187	$1.5 \times 10^{-4**}$
	3R	2R	-0.444	-0.772	-0.115	$1.67 \times 10^{-3**}$
	3R	2L	-0.045	-0.363	0.274	0.999
	3R	3L	0.083	-0.268	0.434	0.985
	X	2R	-1.081	-1.402	-0.760	$< 10^{-16**}$
	X	2L	-0.682	-0.994	-0.371	$8.14 \times 10^{-9**}$
	X	3L	-0.554	-0.898	-0.210	$6.80 \times 10^{-5**}$
	X	3R	-0.638	-0.970	-0.305	$7.74 \times 10^{-7**}$
	X	4	-0.574	-1.348	0.200	0.279
	4	2L	-0.108	-0.876	0.660	0.999
	4	2R	-0.507	-1.279	0.265	0.419
	4	3R	-0.063	-0.840	0.714	1.000
	4	3L	0.020	-0.762	0.802	1.000
<i>D. simulans</i>	2R	2L	0.064	-0.353	0.480	0.998
	3L	2L	0.444	0.027	0.862	0.029*
	3L	2R	0.380	-0.009	0.770	0.060
	3R	2R	-0.170	-0.570	0.231	0.832
	3R	2L	-0.106	-0.533	0.322	0.981
	X	2L	-0.080	-0.484	0.324	0.993
	X	2R	-0.144	-0.519	0.231	0.884
	X	3L	-0.524	-0.900	-0.148	$1.06 \times 10^{-3**}$
	X	3R	0.026	-0.362	0.413	1.000
	X	4	1.023	-0.047	2.092	0.070
	3R	3L	-0.550	-0.951	-0.149	$1.36 \times 10^{-3**}$
	4	2L	-1.102	-2.187	-0.018	0.044*
	4	2R	-1.166	-2.241	-0.092	0.024*
	4	3L	-1.547	-2.621	-0.472	$6.11 \times 10^{-4**}$
	4	3R	-0.997	-2.075	0.082	0.089

* $P < 0.05$, ** $P < 0.01$

Table S28: Tukey's HSD test for number of duplications per mapped bp by chromosome

Species	Chromosome	vs. Chromosome	difference	lower	upper	Adjusted P -value
<i>D. yakuba</i>	2R	2L	2.955×10^{-7}	-2.506×10^{-7}	8.415×10^{-7}	0.620
	3L	2L	-2.049×10^{-7}	-7.510×10^{-7}	3.411×10^{-7}	0.885
	3R	2L	-1.104×10^{-7}	-6.565×10^{-7}	4.356×10^{-7}	0.992
	3L	2R	-5.004×10^{-7}	-1.046×10^{-6}	4.566×10^{-8}	0.092
	3R	2R	-4.059×10^{-7}	-9.519×10^{-7}	1.401×10^{-7}	0.267
	3R	3L	9.449×10^{-8}	-4.516×10^{-7}	6.405×10^{-7}	0.996
	X	2L	3.587×10^{-7}	-1.873×10^{-7}	9.047×10^{-7}	0.404
	X	2R	6.323×10^{-8}	-4.828×10^{-7}	6.093×10^{-7}	0.999
	X	3L	5.636×10^{-7}	1.756×10^{-8}	1.110×10^{-6}	0.039*
	X	3R	4.691×10^{-7}	-7.692×10^{-8}	1.015×10^{-6}	0.135
	X	4	-6.273×10^{-7}	-1.217×10^{-6}	-3.750×10^{-8}	0.030*
	4	2L	9.860×10^{-7}	3.962×10^{-7}	1.576×10^{-6}	$4.969 \times 10^{-05**}$
	4	2R	6.905×10^{-7}	1.007×10^{-7}	1.280×10^{-6}	0.012*
	4	3L	1.191×10^{-6}	6.011×10^{-7}	1.781×10^{-6}	$1.766 \times 10^{-6**}$
	4	3R	1.096×10^{-6}	5.066×10^{-7}	1.686×10^{-6}	$7.319 \times 10^{-6**}$
<i>D. simulans</i>	2R	2L	3.962×10^{-7}	-4.214×10^{-8}	8.344×10^{-7}	0.101
	3L	2L	3.565×10^{-7}	-8.180×10^{-8}	7.948×10^{-7}	0.180
	3R	2L	-6.753×10^{-8}	-5.058×10^{-7}	3.708×10^{-7}	0.998
	3L	2R	-3.966×10^{-8}	-4.780×10^{-7}	3.986×10^{-7}	1.000
	3R	2R	-4.637×10^{-7}	-9.020×10^{-7}	-2.538×10^{-8}	0.032*
	3R	3L	-4.240×10^{-7}	-8.623×10^{-7}	1.428×10^{-8}	0.064
	X	2L	1.107×10^{-6}	6.687×10^{-7}	1.545×10^{-6}	$5.742 \times 10^{-10**}$
	X	2R	7.109×10^{-7}	2.726×10^{-7}	1.149×10^{-6}	$1.0537 \times 10^{-4**}$
	X	3L	7.505×10^{-7}	3.123×10^{-7}	1.189×10^{-6}	$3.574 \times 10^{-5**}$
	X	3R	1.175×10^{-6}	7.363×10^{-7}	1.613×10^{-6}	$5.891 \times 10^{-11**}$
	X	4	-4.977×10^{-7}	-9.417×10^{-7}	-5.369×10^{-8}	0.019*
	4	2L	1.605×10^{-6}	1.161×10^{-6}	2.049×10^{-6}	$3.675 \times 10^{-14**}$
	4	2R	1.209×10^{-6}	7.646×10^{-7}	1.653×10^{-6}	$3.144 \times 10^{-11**}$
	4	3L	1.248×10^{-6}	8.042×10^{-7}	1.692×10^{-6}	$8.245 \times 10^{-12**}$
	4	3R	1.672×10^{-6}	1.228×10^{-6}	2.116×10^{-6}	$2.420 \times 10^{-14**}$

* $P < 0.05$, ** $P < 0.01$

Table S29: Duplications confirmed via split read mapping with Pindel

Species	Chromosome	Confirmed	Total	Percent Confirmed
<i>D. yakuba</i>	2L	42	334	12.5%
	2R	26	294	8.8%
	3L	31	225	13.7%
	3R	45	256	17.6%
	X	32	279	11.5%
	4	3	27	11.1%
<i>D. simulans</i>	2L	30	154	19.5%
	2R	39	200	19.5%
	3L	29	198	14.6%
	3R	29	178	16.3%
	X	31	231	13.4%
	4	4	14	28.6%

Table S30: Breakpoints Reconstructed

Species	Min Size (bp)	Chromosome	Reconstructed	Total	Percent Reconstructed
<i>D. yakuba</i>	0	2L	145	338	42.9
		2R	133	296	44.9
		3L	78	237	32.9
		3R	97	260	37.3
		X	81	284	28.5
		4	8	27	29.6
	325	2L	142	256	55.5
		2R	133	253	52.6
		3L	75	170	44.1
		3R	95	195	48.7
		X	74	162	45.7
		4	8	21	38.1
	500	2L	138	229	60.3
		2R	131	231	56.7
		3L	72	150	48.0
		3R	93	174	53.4
		X	66	130	50.8
		4	8	20	40.0
	1000	2L	127	194	65.5
		2R	124	209	59.3
		3L	62	111	55.9
3R		88	150	58.7	
X		58	95	61.1	
4		7	14	50.0	
<i>D. simulans</i>	0	2L	87	157	55.4
		2R	102	200	51.0
		3L	85	198	42.9
		3R	77	178	43.3
		4	3	14	21.4
		X	106	231	45.9
	325	2L	85	118	72.0
		2R	100	171	58.5
		3L	85	162	52.5
		3R	76	140	54.3
		4	3	8	37.5
		X	102	177	57.6
	500	2L	84	109	77.1
		2R	98	146	67.1
		3L	82	147	55.8
		3R	74	115	64.3
		4	3	6	50.0
		X	98	154	63.6
	1000	2L	71	87	81.6
		2R	85	114	74.6
		3L	76	128	59.4
3R		67	88	76.1	
4		2	2	100.0	
X		77	110	70.0	

Table S31: Duplications with increased coverage compared to reference

Species	total	>25%	>50%	>75%
<i>D. yakuba</i>	1442	833	646	430
<i>D. simulans</i>	978	641	507	321

Supplementary Figures

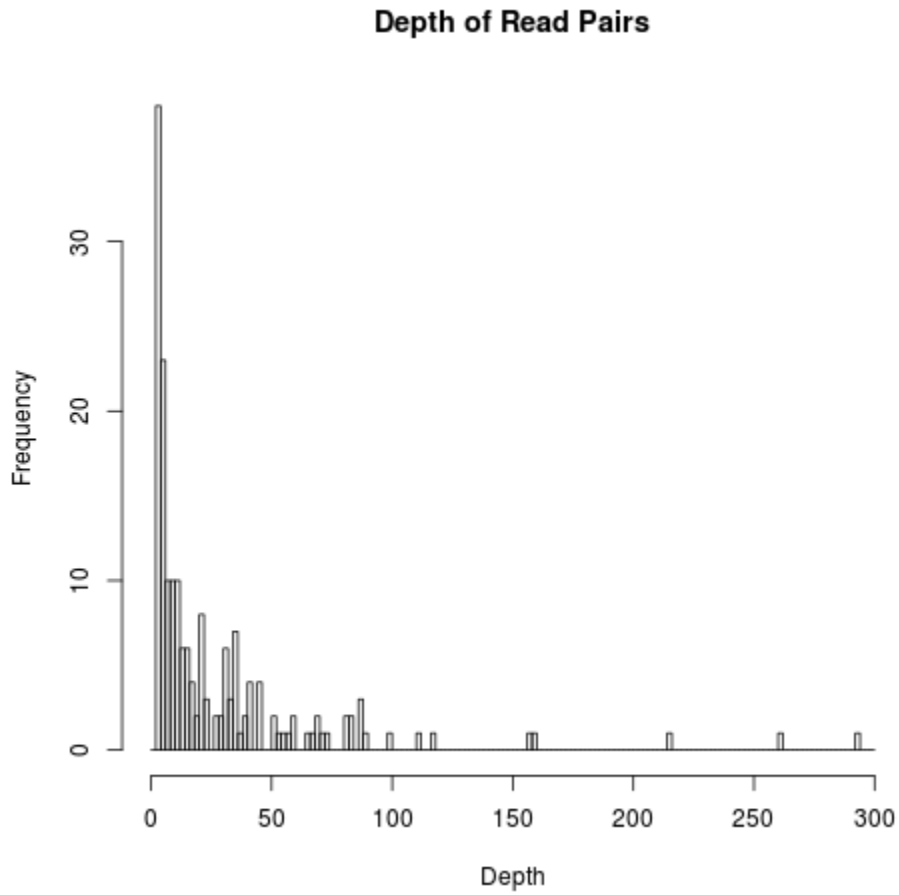


Figure S1: Histogram of read pair depth indicating a tandem duplication for sample strain CY20A. Number of read pairs is highly skewed and ranges from 3-300 read pairs supporting each event. Mean depth is 22.3, and median of 11 read pairs.

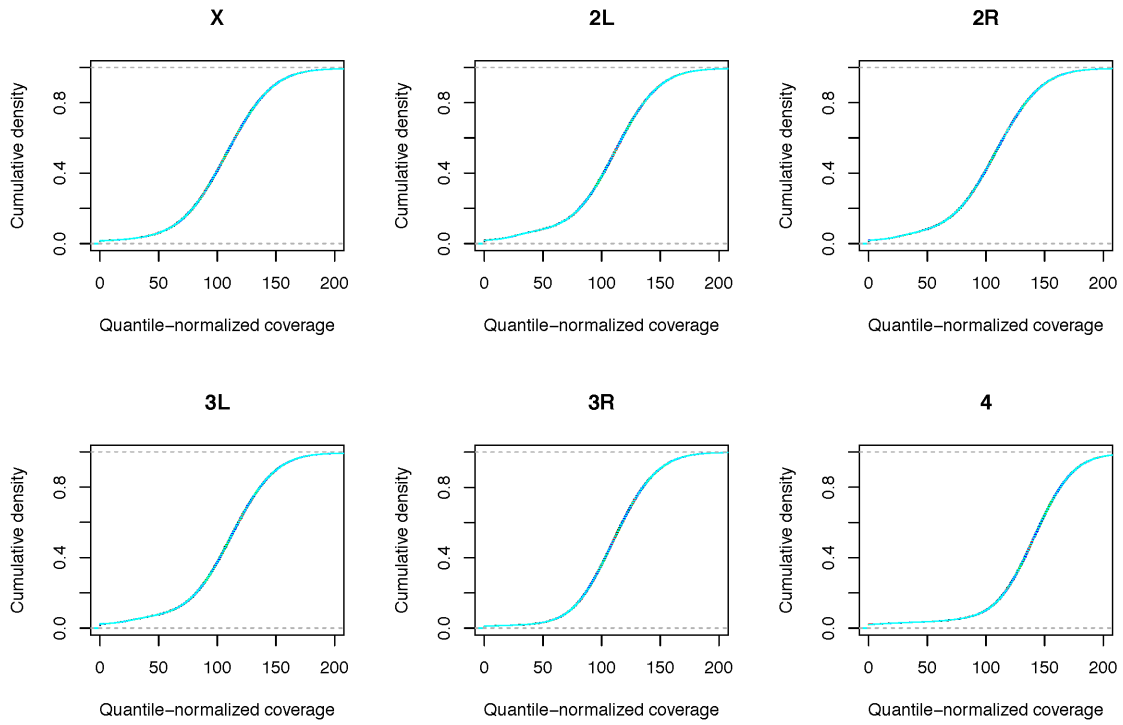


Figure S2: Cumulative distribution plots of the result of quantile-normalization of raw sequence coverage for the *D. simulans* samples. All 21 samples are plotted, each with an arbitrary color. Compared to the variable median raw coverage values shown in Table S4, the quantile normalization procedure results in the same distribution of coverage for all samples.

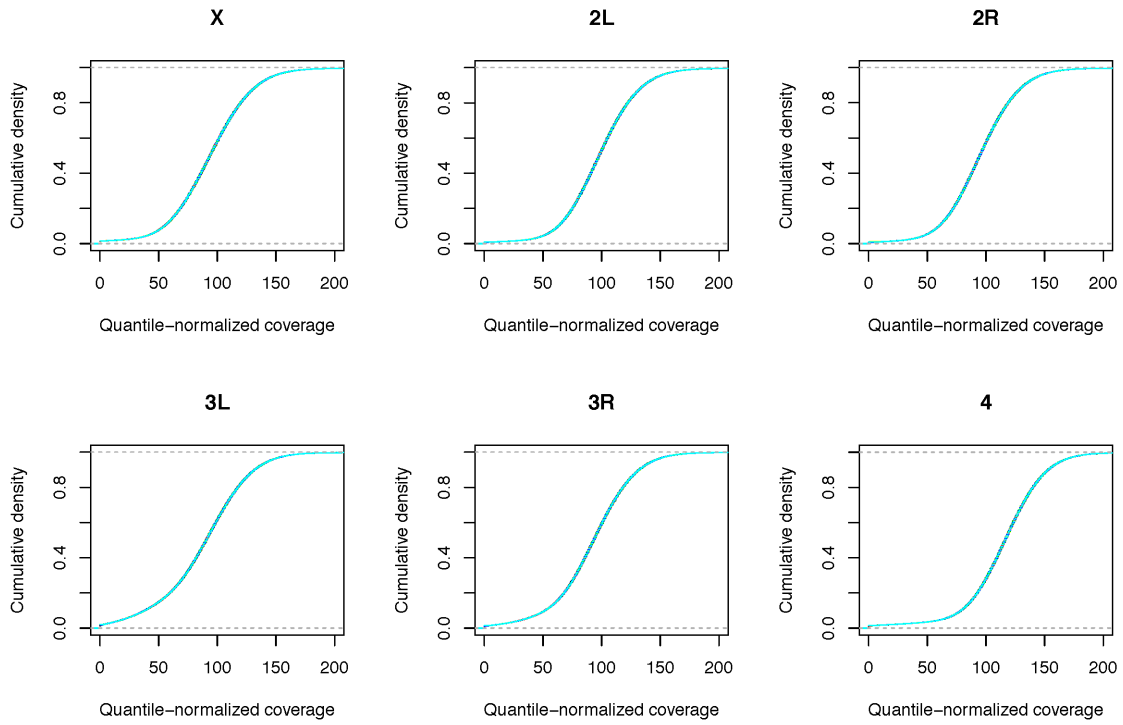


Figure S3: Cumulative distribution plots of the result of quantile-normalization of raw sequence coverage for the *D. yakuba* samples. All 21 samples are plotted, each with an arbitrary color. Compared to the variable median raw coverage values shown in Table S4, the quantile normalization procedure results in the same distribution of coverage for all samples.

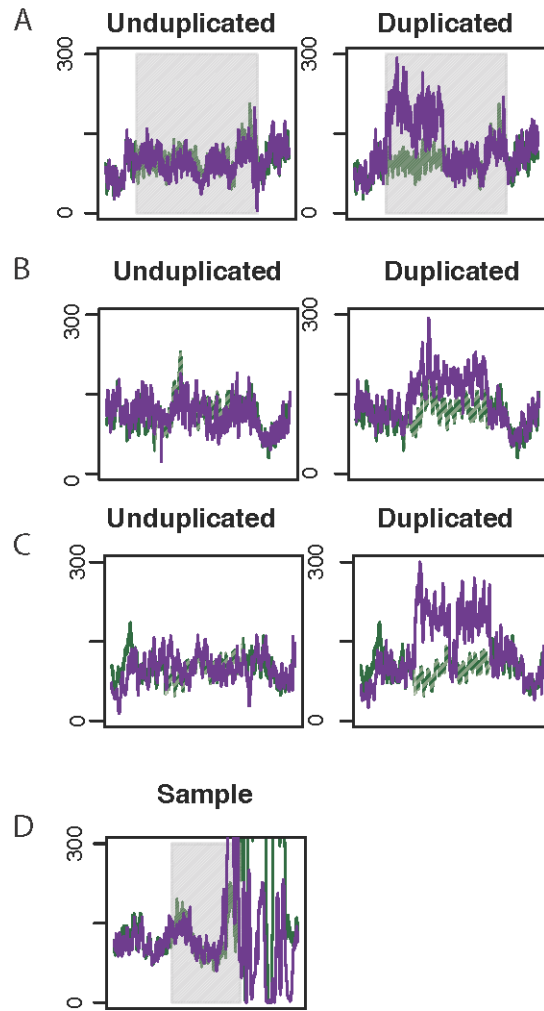


Figure S4: Cases where automated detection of duplicates using coverage becomes problematic. A. A duplication has occurred but coverage does not increase for the full variant length. Possible explanations include subsequent deletion, duplication combined with gene conversion in an adjacent region, or TE movement combined with duplication. B. Coverage increases, but there remains substantial overlap between sample and reference coverage. Modest coverage increases such as these could putatively be hemizygous duplicates, high variance in coverage, or other factors. C. A region is duplicated with subsequent deletion in the interior of one copy. D. Reference and sample variance are typical in one region but variance is magnified in an adjacent region. Automated detection for the typical region may be problematic due to an inability to properly estimate HMM parameters due to the abnormally high variance in the same window.

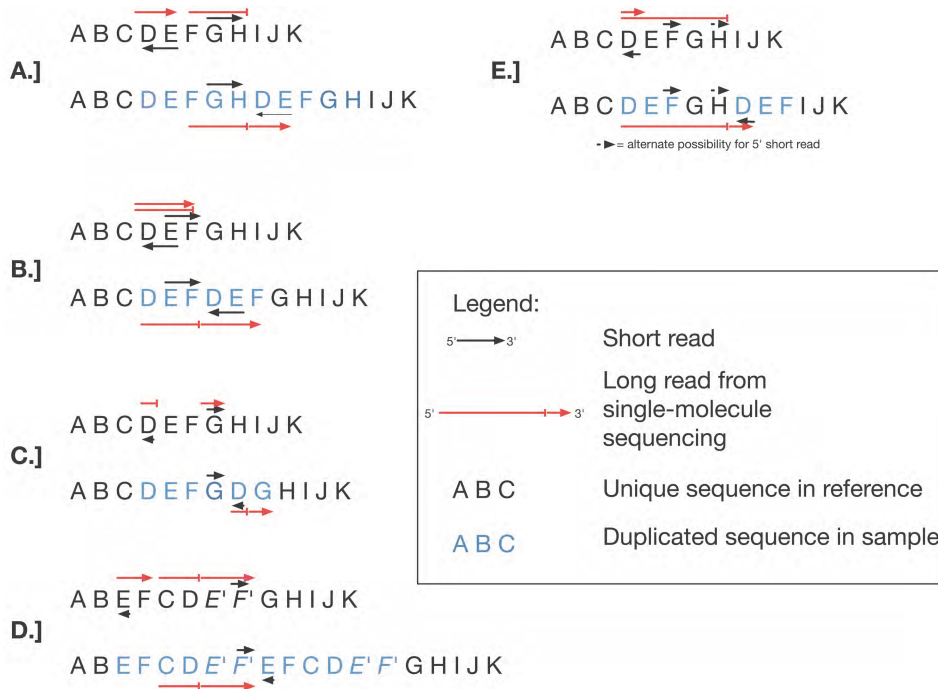


Figure S5: Confirmation of tandem duplications using single-molecule sequencing. We considered five simple breakpoint structures resulting from simple tandem duplication events. A.] A simple tandem duplication. Short reads (black arrows) from this type of breakpoint map in a divergent orientation, with reads aligning to different strand and pointing (5' to 3') away from each other (Cridland and Thornton 2010) when aligned to the reference. A long read (red arrow) spanning such a breakpoint will align discontinuously to the reference, with the fragment from the 3' section of the breakpoint aligning to the reference upstream of where the fragment from the 5' section of the breakpoint aligns. These fragments are expected to align to the loci where the divergently-oriented reads aligned. B.] When the long read is long relative to the length of the duplication, the entire duplication event may be captured in a single read. In this case, the long read will contain two alignments to the region flanked by divergently-oriented short reads. C.] The case of an incomplete duplication, where markers E and F are deleted from the tandem duplicate. In this case, 5' fragment of a long read will align to the 5' segment of the reference containing divergently-oriented short reads (*e.g.* short reads aligned to the minus strand), and the 3' fragment will align to the 3' cluster of divergently-oriented reads (which are aligned to the plus strand). The two fragments of the long read will align to the same strand in the same orientation. D.] The case of a tandem duplication involving semi-repetitive sequence. Here, the regions EF and E'F' in the reference are assumed to be similar, but not identical, in sequence, such that short reads may align uniquely to positions differentiating the two loci. A long read spanning the repetitive segment will result in a fragment aligning twice to the reference. This multiply-mapping segment will cover both regions containing divergently-oriented short reads. E.] The case of a tandem duplication separated by spacer sequence. For this case, there are two possible configurations for divergently-oriented short reads, and a long read spanning the novel breakpoint will contain two different regions mapping to the same part of the reference sequence.

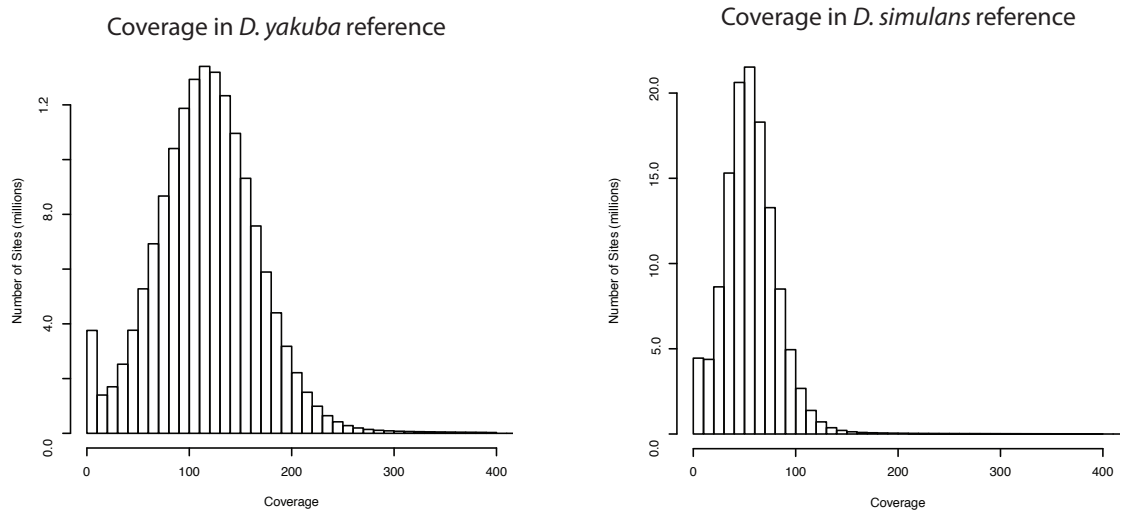
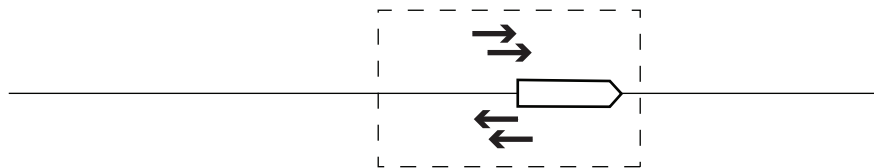


Figure S6: Histogram of raw coverage in the *D. yakuba* and *D. simulans* reference genomes. Sites with coverage higher than 400X not shown. Median coverage in the *D. yakuba* reference was 115X whereas the *D. simulans* reference was sequenced to 55X.

Reference



Sample

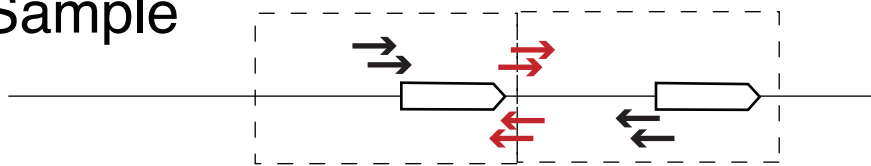


Figure S7: Unique Reads at duplication breakpoints. A duplication in the sample strain (below) is used to generate paired-end sequencing libraries. Read pairs interior to duplication boundaries map uniquely to the genome. However read pairs which overlap with duplication boundaries (red) contain unique sequence which is not present in the reference and remain unmapped. Breakpoint sequence can be assembled *de novo* from unmapped partners of mapped reads.

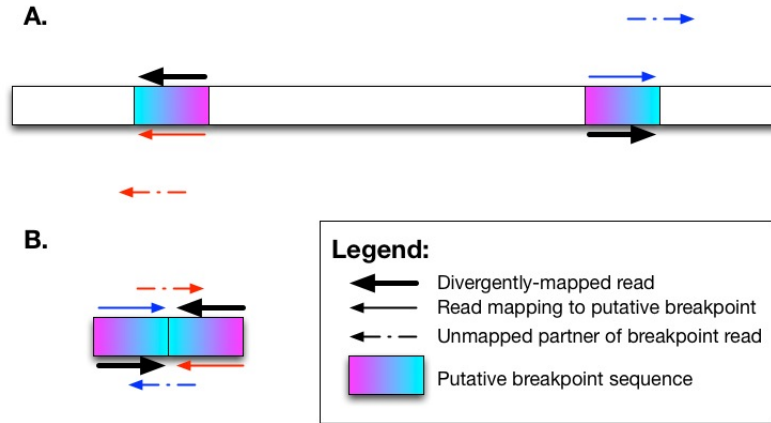


Figure S8: Cartoon of *de novo* assembly procedure. (a) We mined the alignment archives (bam files) for both the divergently-mapping reads (thick black arrows) and the mapped/unmapped pairs whose mapped reads align to the putative breakpoint regions. (b) Once assembled using *phrap*, a single contig with reads spanning the novel junction of the breakpoint confirms the detection of a tandem duplication with a simple breakpoint sequence.

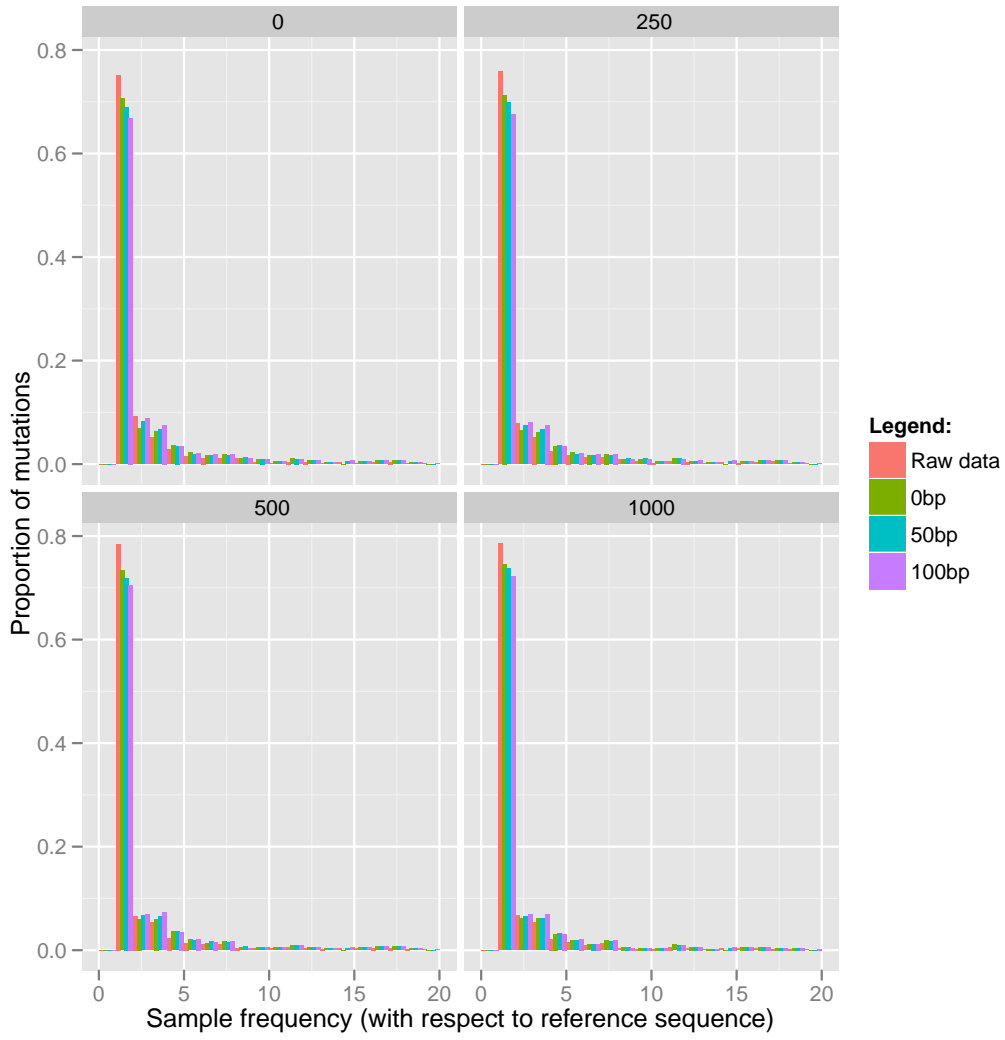


Figure S9: SFS for confirmed breakpoints in *D. yakuba*

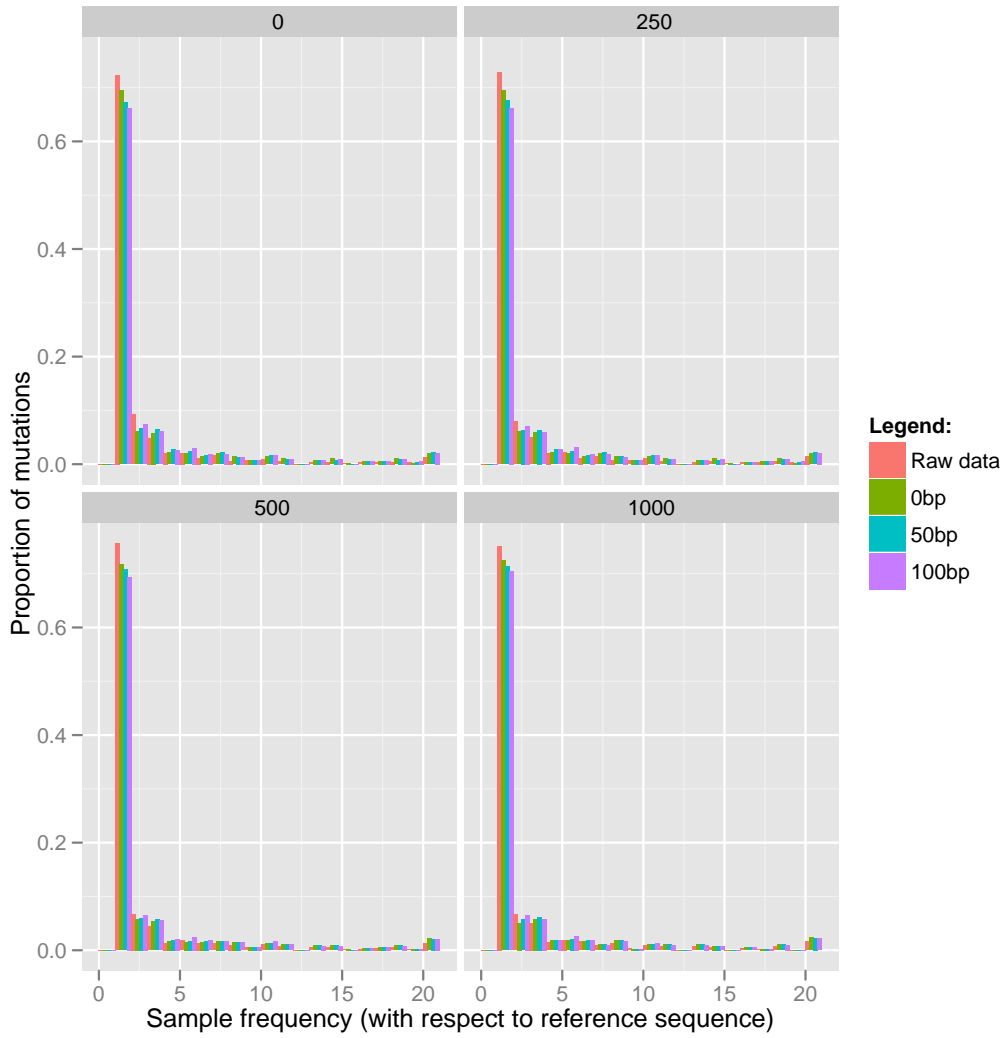


Figure S10: SFS for confirmed breakpoints in *D. simulans*